Sources of ultra-high-energy cosmic rays and how to infer them from data

Teresa Bister
Erice, July 2024

Radboud University

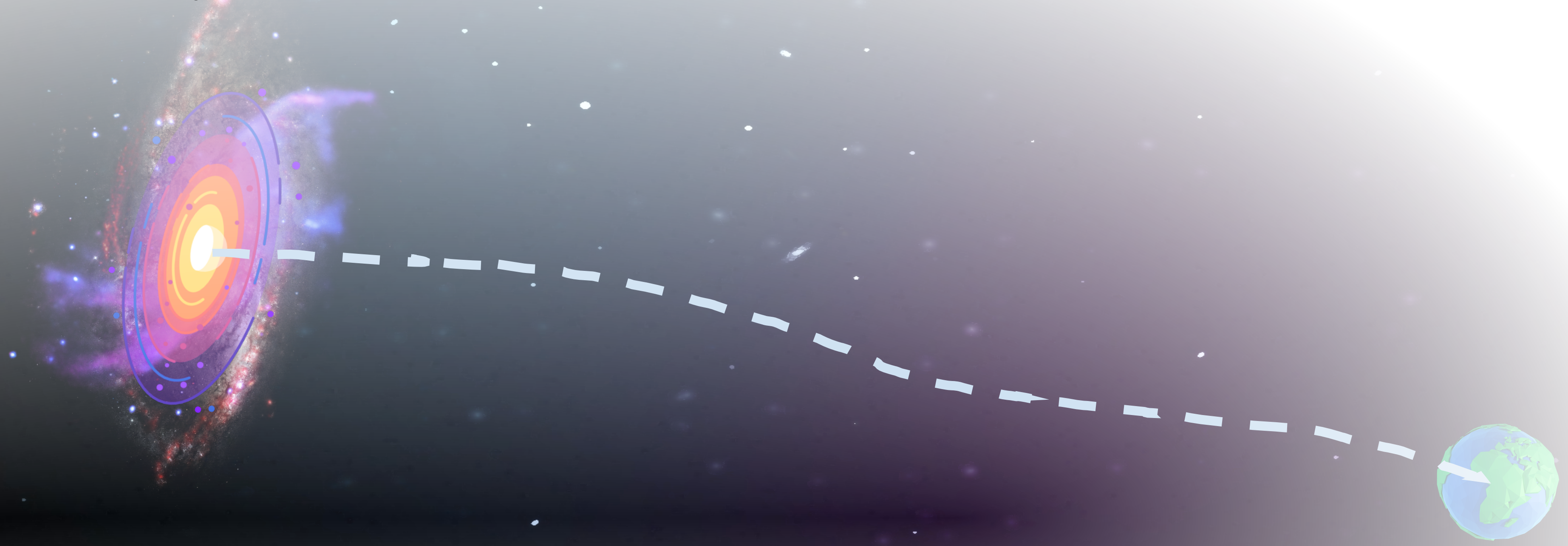

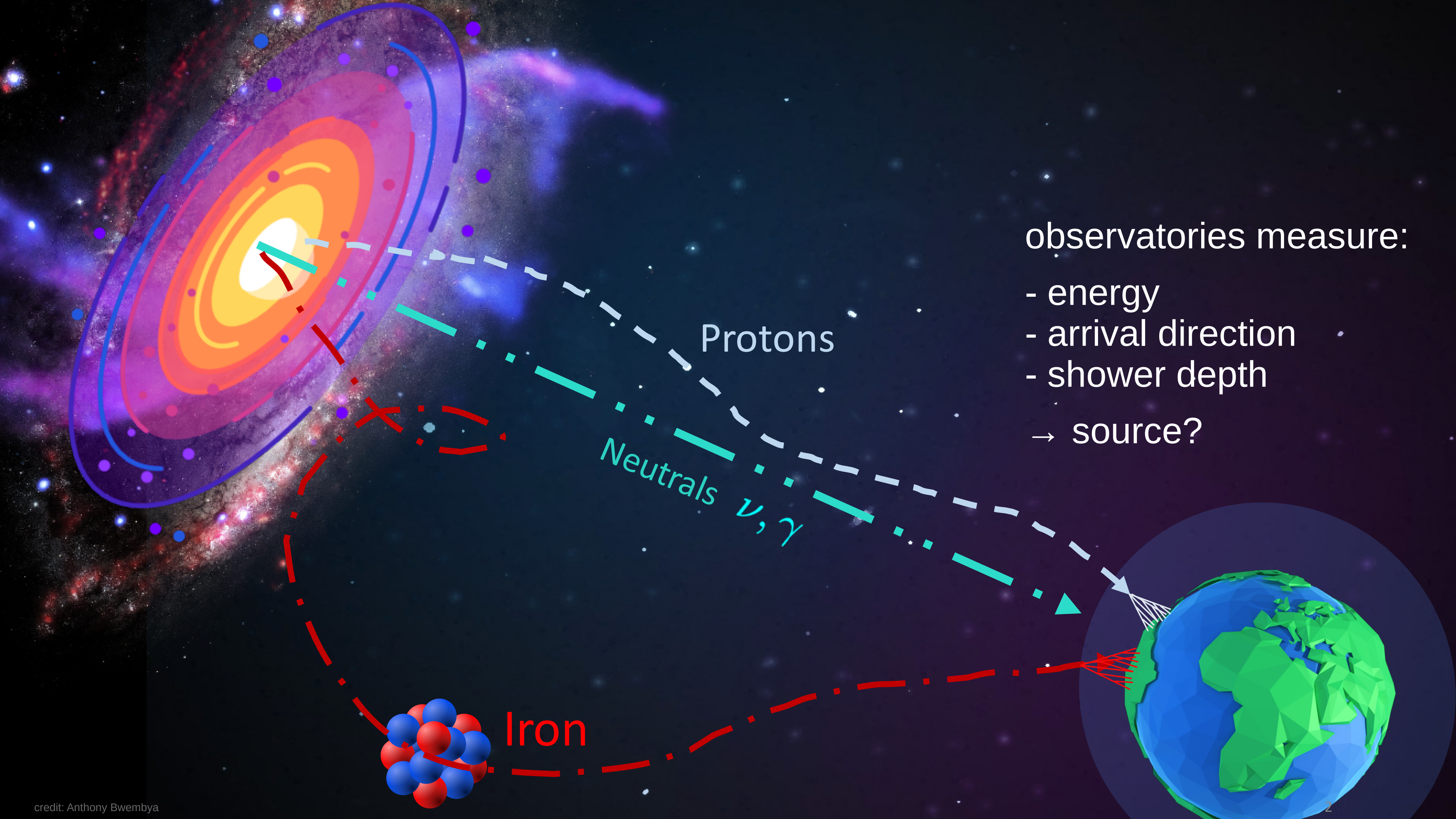

credit: Anthony Bwembya

Modeling UHECRs from sources to detection

source distribution

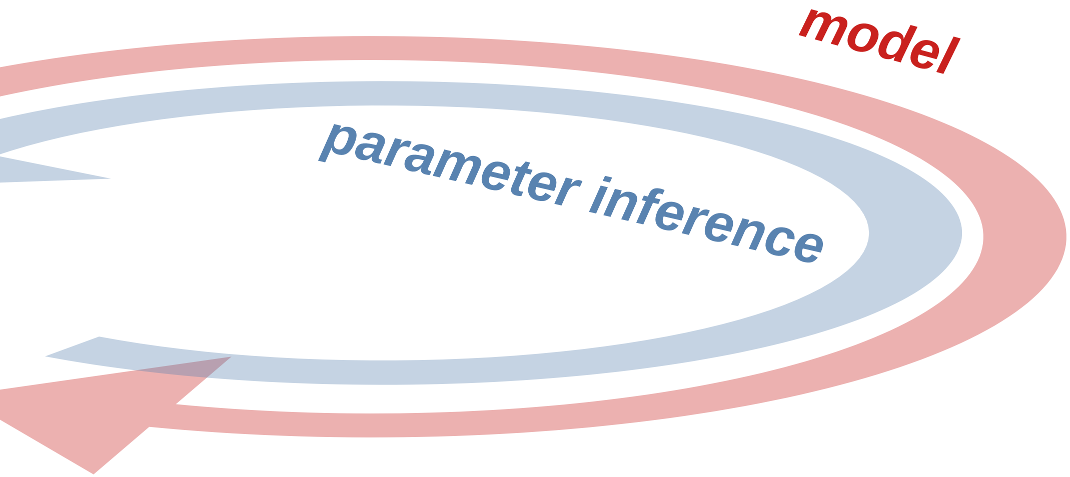

compare to data

- energy spectrum
- mass composition
- arrival directions
- (multimessenger)

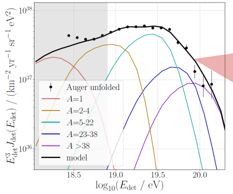

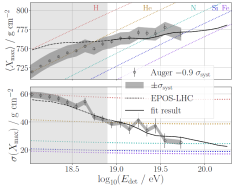

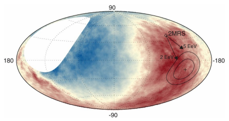

Modeling UHECR sources

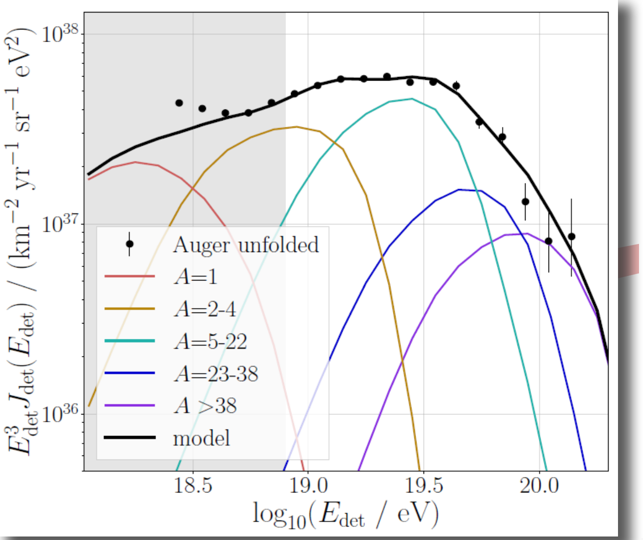

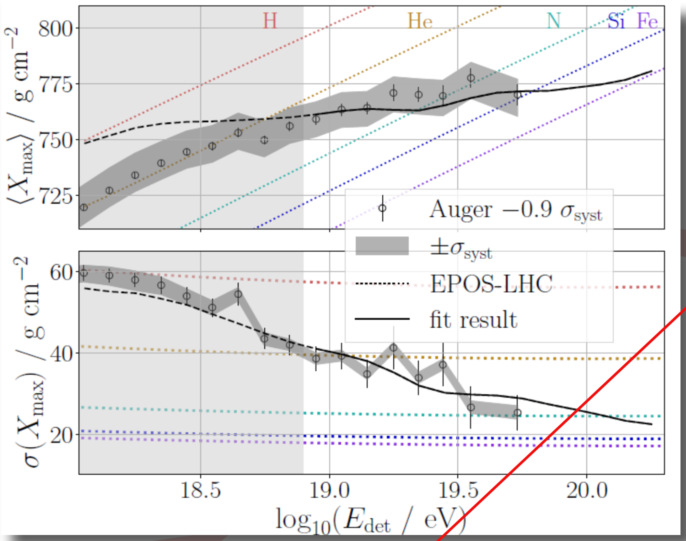

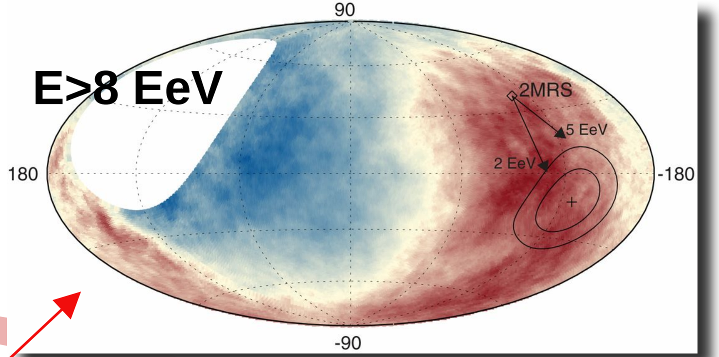

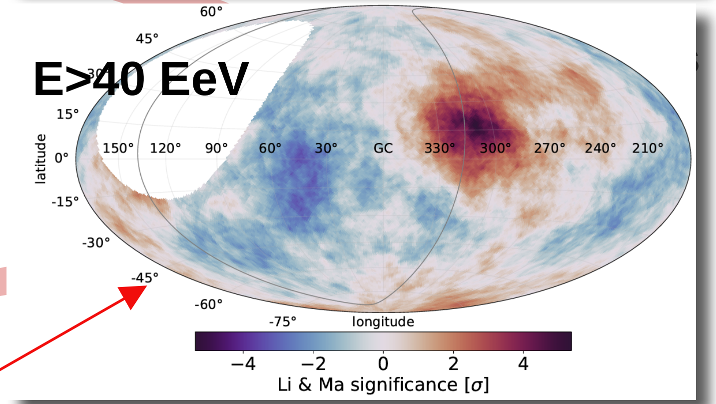

compare to data

- energy spectrum
- mass composition (often X_{max})
- arrival directions (events *or* large-scale / smaller scale anisotropies *or* correlations)
- (multimessenger)

Modeling UHECRs from sources to detection

source distribution

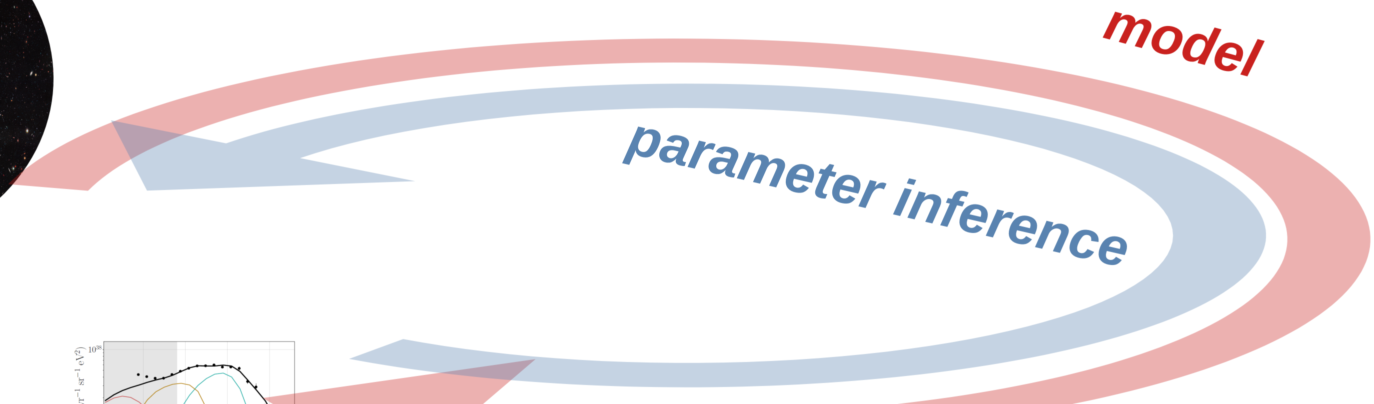

compare to data

- energy spectrum
- mass composition
- arrival directions
- (multimessenger)

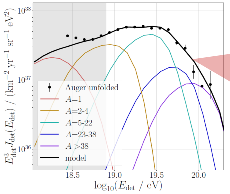

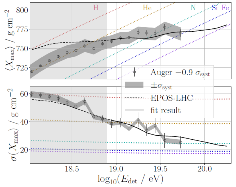

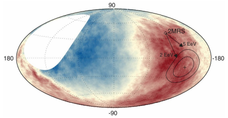

Modeling UHECRs from sources to detection

source distribution

injection

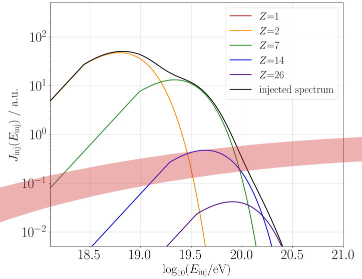

propagation through extragalactic space

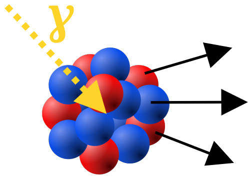

SimProp SIRENTE

CRPropa

extragalactic magnetic fields

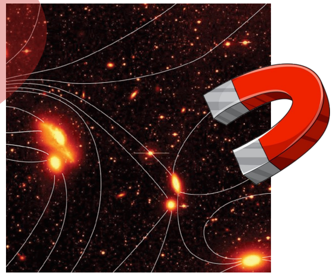

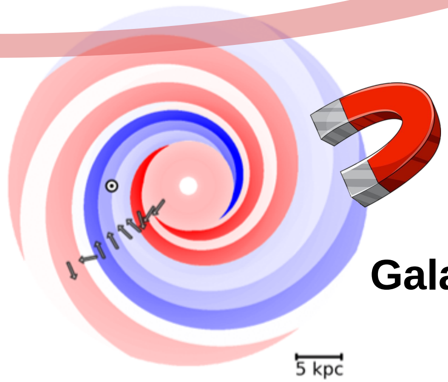

Galactic magnetic fields

compare to data

- energy spectrum
- mass composition
- arrival directions
- (multimessenger)

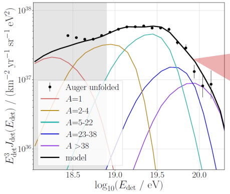

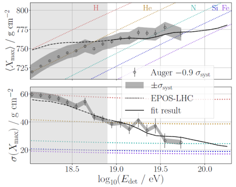

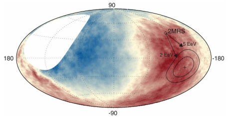

Pierre Auger Collaboration JCAP05(2023)024

Combined fit of spectrum and composition

source distribution

homogeneous

injection

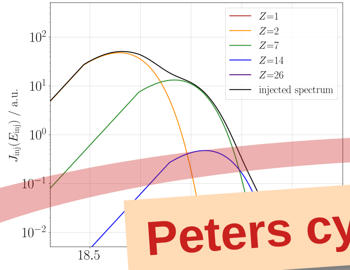

Peters cycle

propagation through extragalactic space

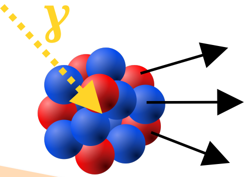

SimProp SIRENTE

CRPropa

1-dimensional

extragalactic magnetic fields

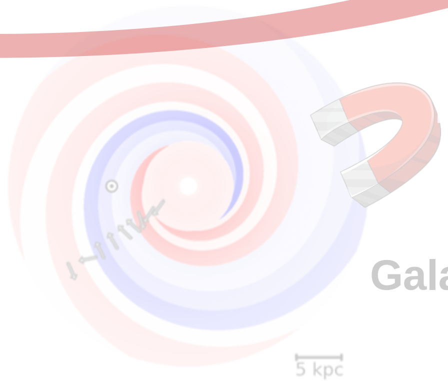

Galactic magnetic fields

compare to data

- energy spectrum
- mass composition
- arrival directions
- (multimessenger)

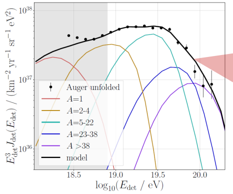

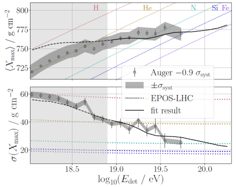

Combined fit of spectrum and composition

- two populations of homogeneous sources
- Peters cycle injection

$$\tilde{Q}_A(E) = \tilde{Q}_{0A} \left(\frac{E}{E_0}\right)^{-\gamma} \begin{cases} 1, & E \le Z_A R_{\rm cut} \\ \exp\left(1 - \frac{E}{Z_A R_{\rm cut}}\right), & E > Z_A R_{\rm cut} \end{cases}$$

spectral index

rigidity cutoff

element contributions

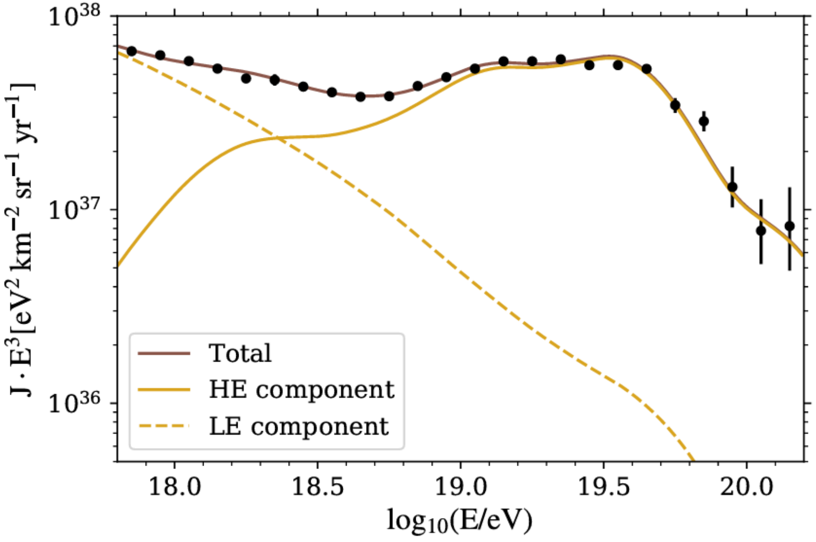

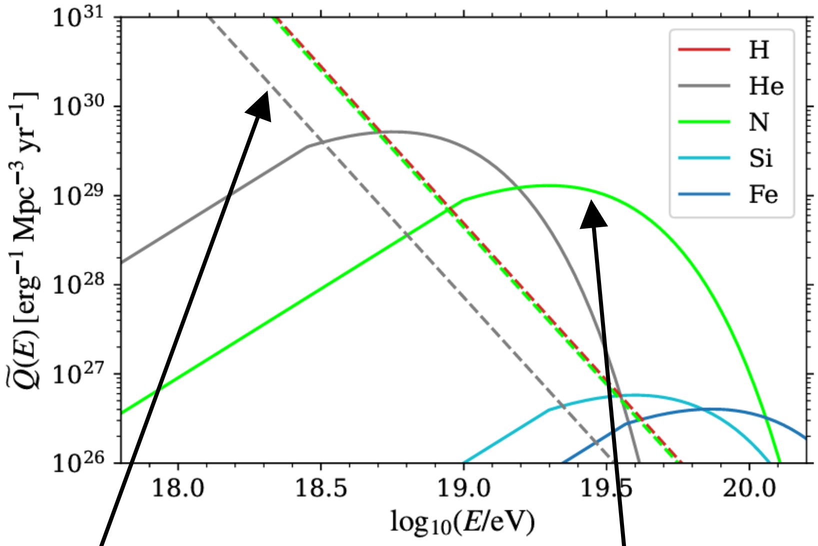

low-energy component:
→ He+N, very soft spectrum
→ rigidity cutoff unconstrained

high-energy component:
→ very hard spectrum γ<0
→ low rigidity cutoff O(1 EeV)

Pierre Auger Collaboration JCAP05(2023)024

Combined fit of spectrum and composition

ankle: transition between populations

conclusions stable with regards to **systematic effects**

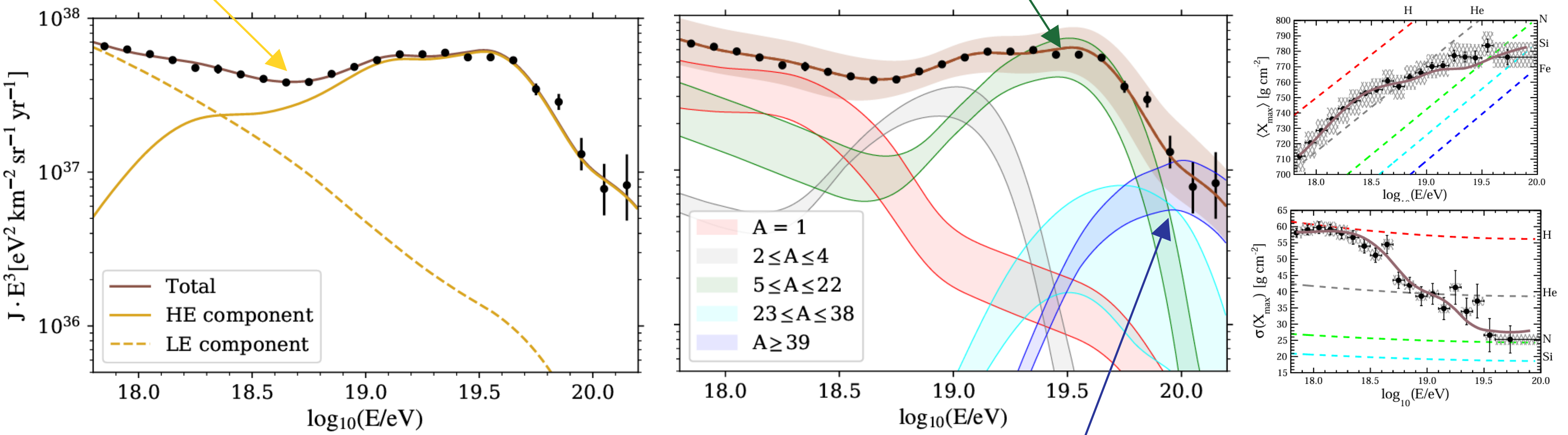

composition becomes heavier → **no light elements at highest energies** ☹️

➡ but, maybe secondaries from in-source interactions or another population, see e.g.
Unger, Farrar, Anchordoqui PRD 92 123001 (2015),
Muzio, Unger, Farrar PRD 100 103008 (2019)
Ehlert, van Vliet, Oikonomou, Winter JCAP 02 022 (2024) ...

Combined fit of spectrum and composition

test cosmological source evolution $\psi(z) \propto (1+z)^m$

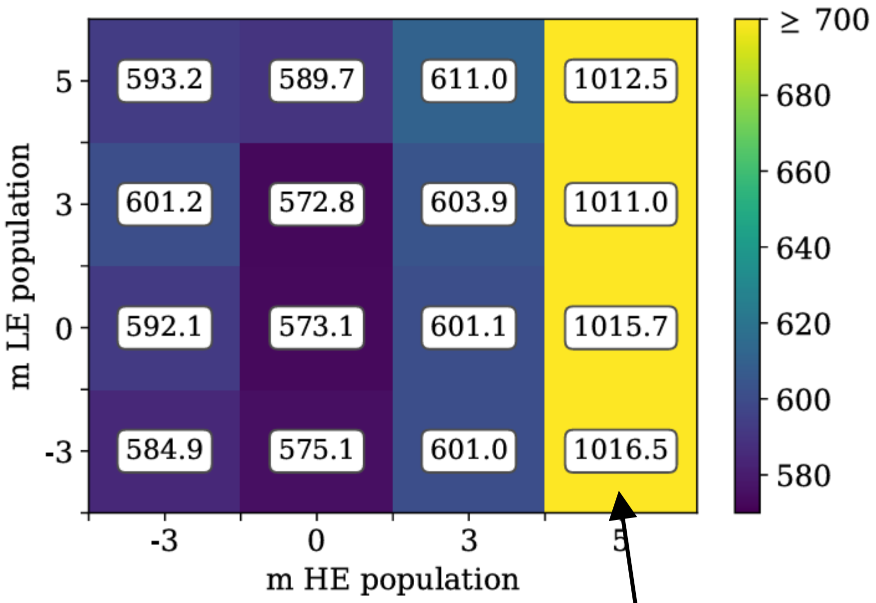

strong evolution of high-energy population disfavored

Combined fit of spectrum and composition

test cosmological source evolution $\psi(z) \propto (1+z)^m$

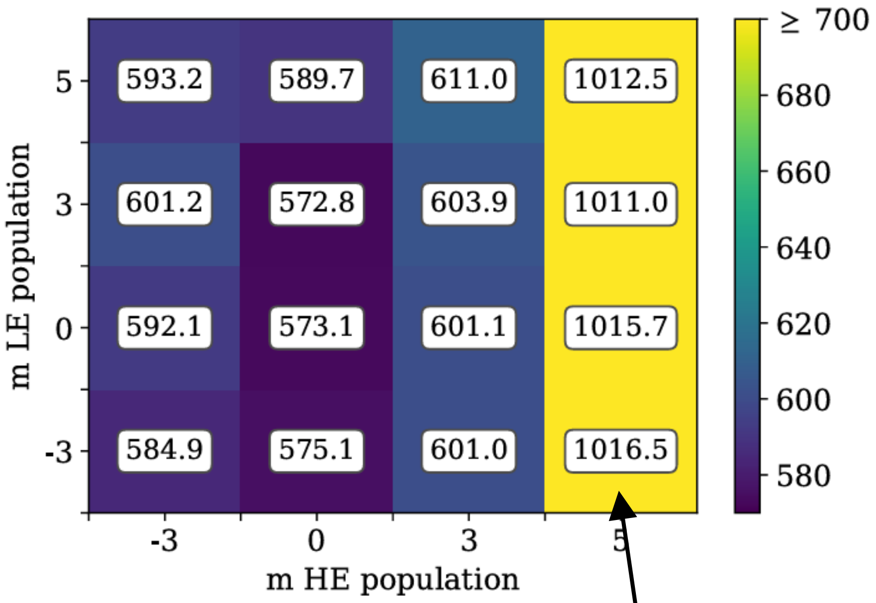

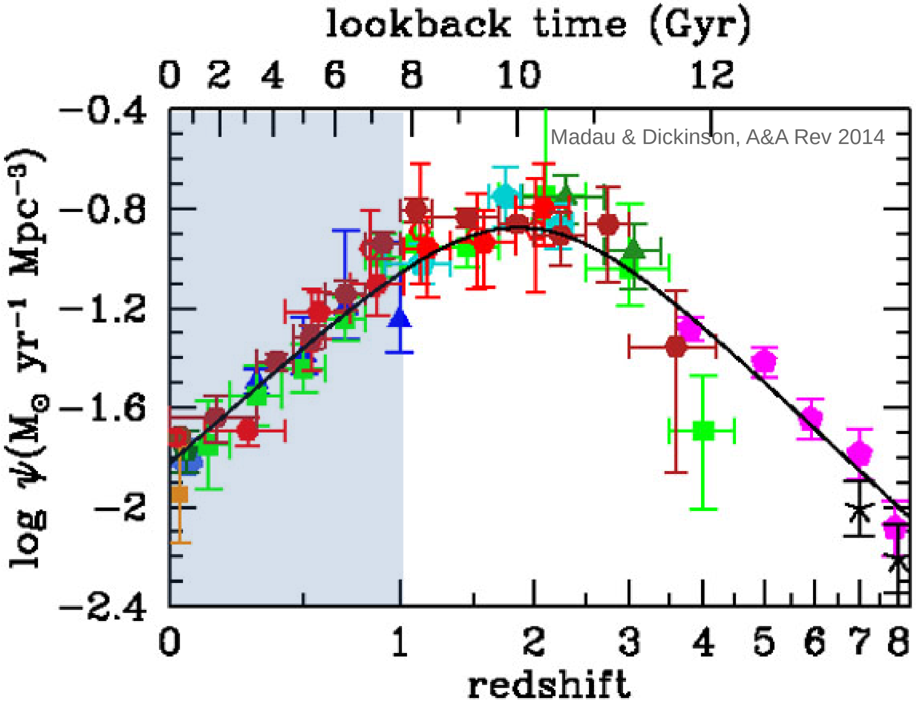

strong evolution of high-energy population disfavored

Combined fit of spectrum and composition

test cosmological source evolution $\psi(z) \propto (1+z)^m$

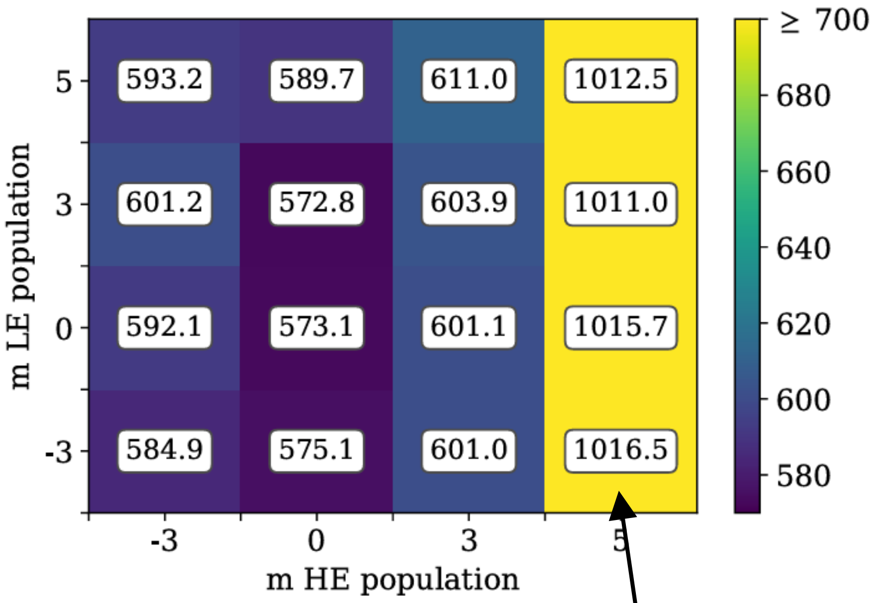

strong evolution of high-energy population disfavored

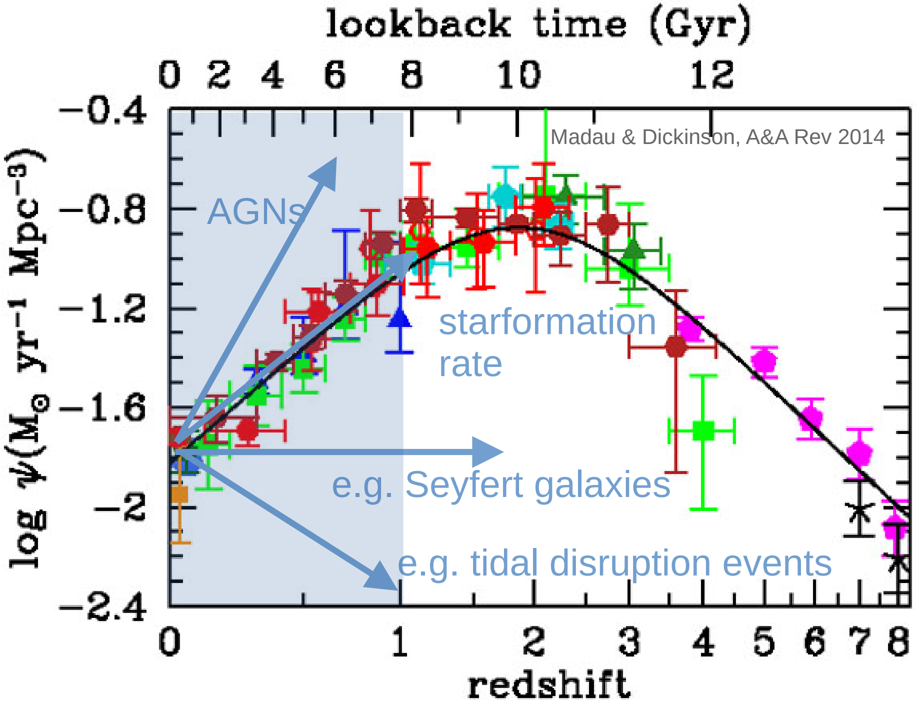

Variations of the injection at the source

source distribution

homogeneous

injection

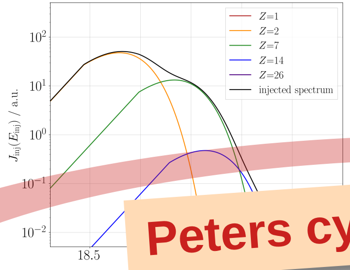

Peters cycle

$$\tilde{Q}_A(E) = \tilde{Q}_{0A} \left(\frac{E}{E_0}\right)^{-\gamma} \begin{cases} 1, & E \le Z_A R_{\mathrm{cut}} \\ \exp\left(1 - \frac{E}{Z_A R_{\mathrm{cut}}}\right), & E > Z_A R_{\mathrm{cut}} \end{cases}$$

spectral index

rigidity cutoff

element contributions

propagation through extragalactic space

extragalactic magnetic fields

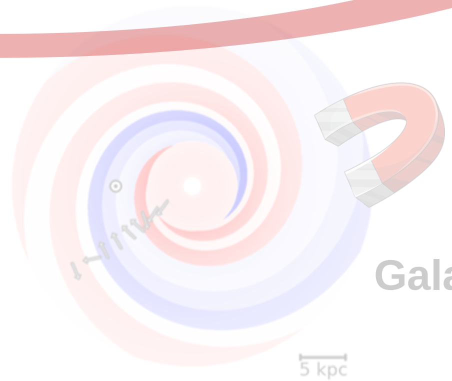

Galactic magnetic fields

compare to data

- energy spectrum
- mass composition
- arrival directions
- (multimessenger)

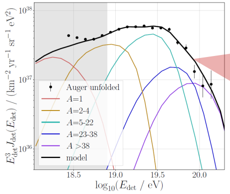

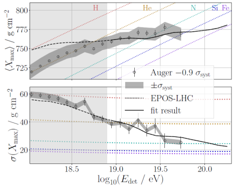

Variations of the injection at the source

source distribution

homogeneous

injection

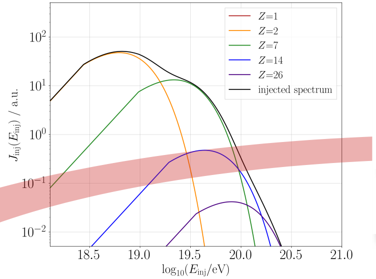

propagation through

spectral index | rigidity cutoff

$$\tilde{Q}_A(E) = \tilde{Q}_{0A} \left(\frac{E}{E_0}\right)^{-\gamma} \begin{cases} 1, & E \le Z_A R_{\mathrm{cut}} \\ \exp\left(1 - \frac{E}{Z_A R_{\mathrm{cut}}}\right), & E > Z_A R_{\mathrm{cut}} \end{cases}$$

element contributions

extragalactic magnetic fields

- *Muzio, Anchordoqui, Unger*, PRD 109 023006 (2024)
  ➔ explore **alternatives to Peters cycle** which might fit better
- *Ehlert, Oikonomou, Unger*, PRD 107, 103045 (2023)
  ➔ explore **variations of maximum rigidity** and find that **sources must be very similar**
- *Eichmann, Kachelrieß, Oikonomou* JCAP 07 006 (2022)
  ➔ explore **individual AGNs** with different properties in a combined fit

compare to data

- energy spectrum
- mass composition
- arrival directions
- (multimessenger)

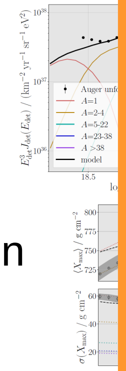

fields

5 kpc

Combined fit including EGMF

source distribution

homogeneous

injection

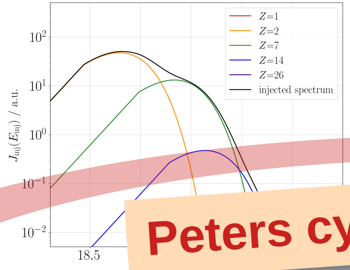

Peters cycle

propagation through extragalactic space

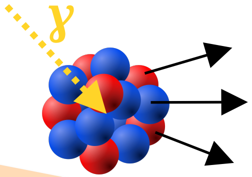

SimProp SIRENTE

CRPropa

1-dimensional

extragalactic magnetic fields

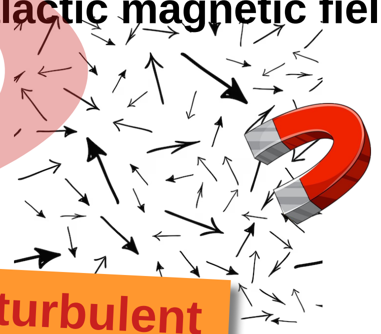

turbulent

compare to data

- energy spectrum
- mass composition
- arrival directions
- (multimessenger)

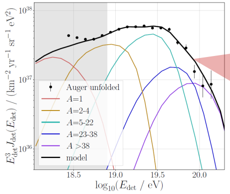

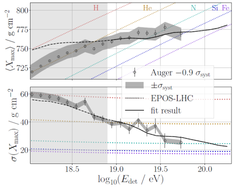

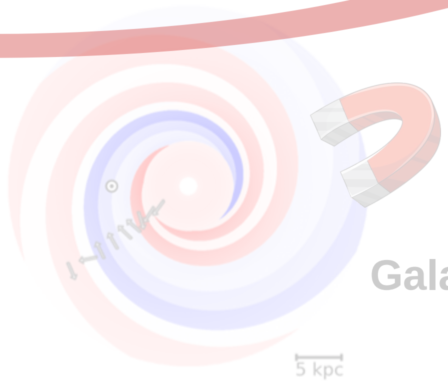

Galactic magnetic fields

Combined fit including EGMF

- extragalactic magnetic field can suppress lower energy particles (diffusion)
- include suppression factor G
  - +2 parameters (critical energy + norm. source density)

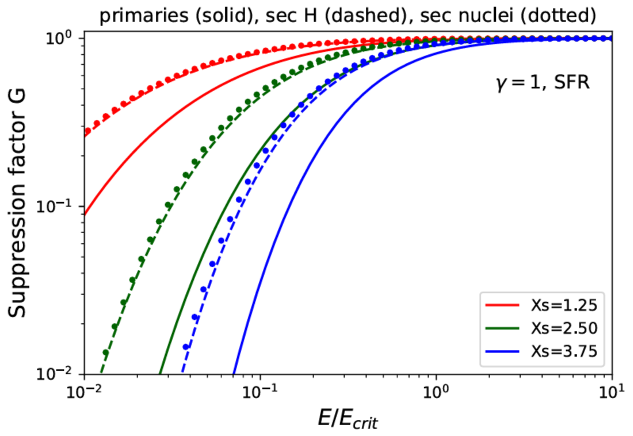

high-energy population injected spectrum now soft!

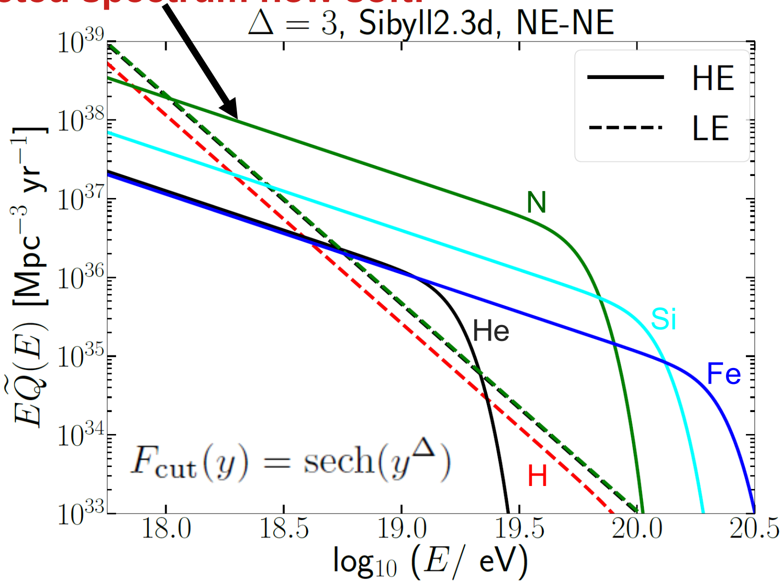

EGMF can have strong effect on injection, but only for:

- steep injection cutoff
- & source densities < 10^{-3} Mpc^{-3}
- & very strong field strengths B~10-200 nG between nearest sources & Earth

➔ then: can reach γ=2

Combined fit including structured EGMF (to spectrum and composition)

source distribution

follows tracer

injection

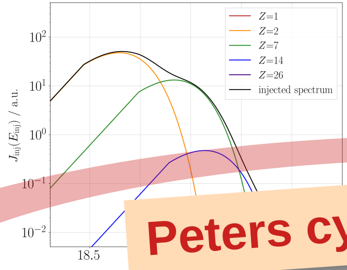

Peters cycle

propagation through extragalactic space

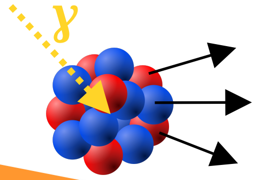

SimProp SIRENTE

CRPropa

3-dimensional

extragalactic magnetic fields

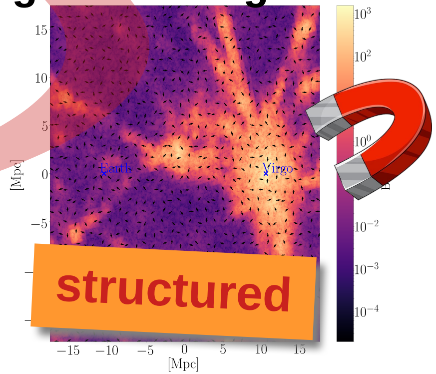

structured

problems: takes very long & not much is measured about EGMF, have to rely on simulations

compare to data

- energy spectrum
- mass composition
- arrival directions
- (multimessenger)

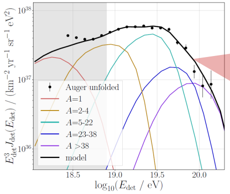

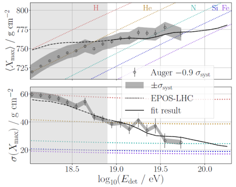

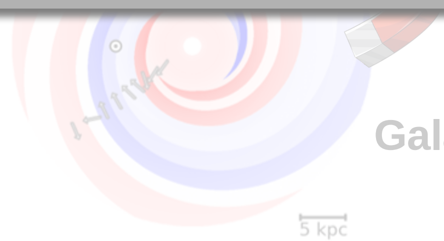

Galactic magnetic fields

Combined fit including structured EGMF (to spectrum and composition)

D. Wittkowski for the Pierre Auger Collaboration
PoS ICRC 2017 563 (preliminary)

- sources follow 2MRs catalog of all galaxies with density ~10^{-4} Mpc^{-3}
- structured EGMF (Dolag model)
  Dolag, Grasso, Springel, Tkachev JCAP 01 009 (2005)

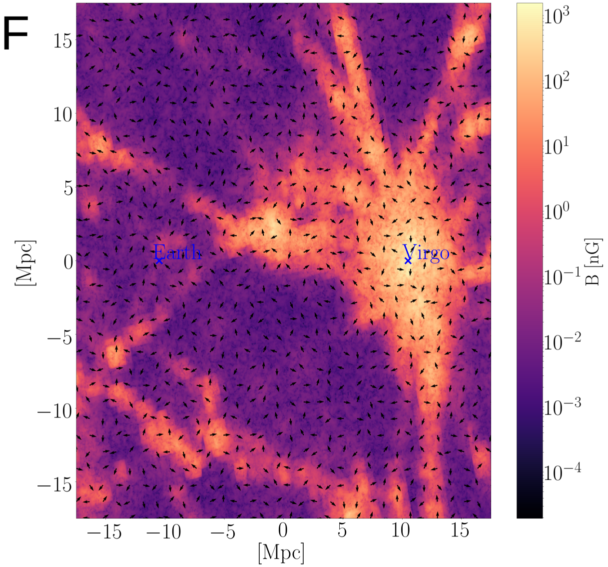

- **results:**
  - ➔ injection parameters sensitive to EGMF
  - ➔ softer injection with EGMF

Lundquist, Merten et al, arXiv:2407.06961

- sources roughly homogeneous (FR0 galaxies with density ~10^{-3} Mpc^{-3})

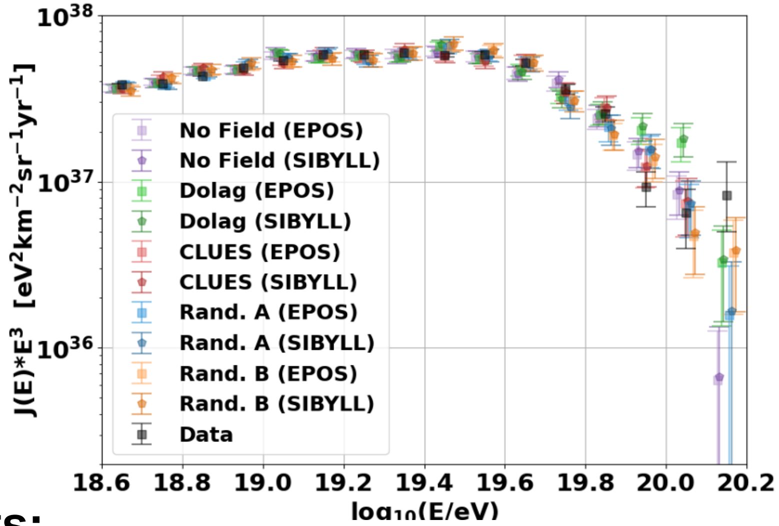

- **results:**
  - ➔ can describe spectrum & composition with any EGMF model

Bister & Farrar, ApJ 966 71 2024

Include arrival directions: large-scale

source distribution

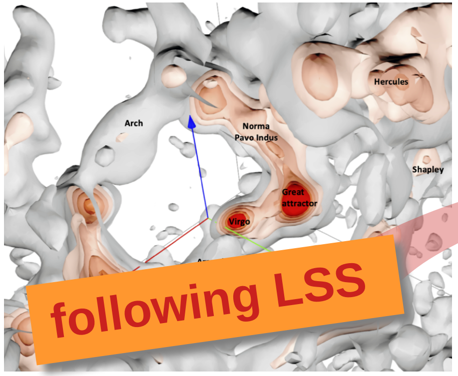

following LSS

injection

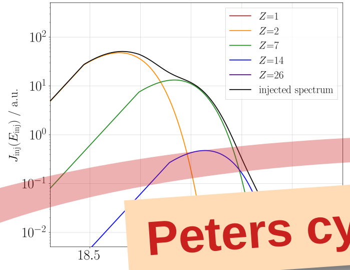

Peters cycle

propagation through extragalactic space

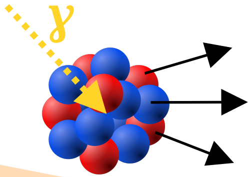

SimProp SIRENTE

CRPropa

1-dimensional

extragalactic magnetic fields

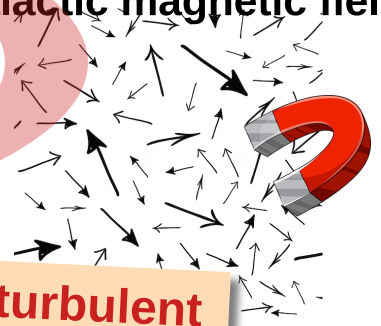

turbulent

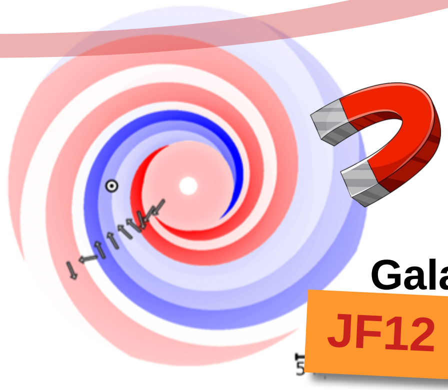

Galactic magnetic fields

JF12

compare to data

- energy spectrum
- mass composition
- arrival directions
- (multimessenger)

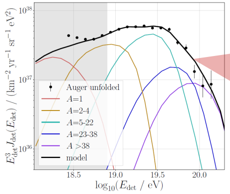

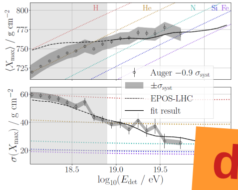

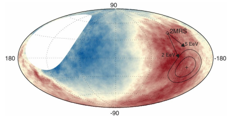

dipole
E>8 EeV

Arrival directions E>8 EeV

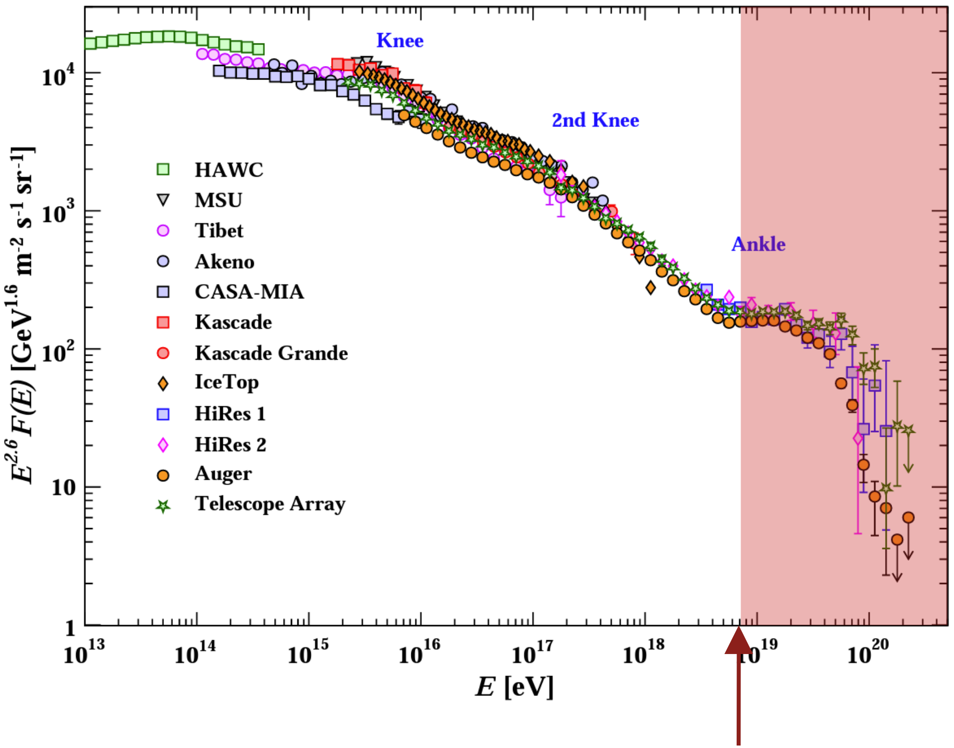

dipole > 8 EeV, >5σ

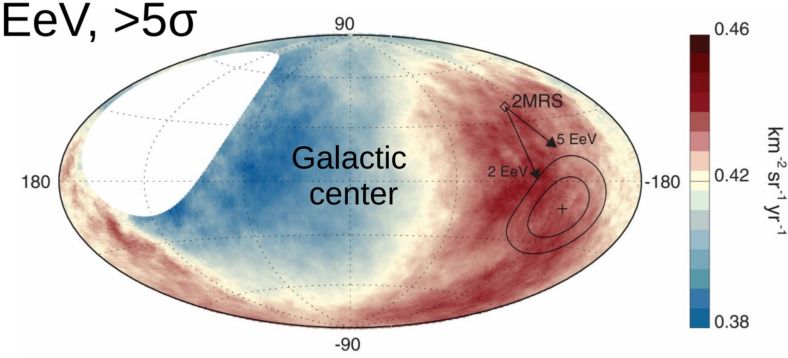

- amplitude ~ 7%, rising with the energy
  - no significant quadrupole or higher moments
- phase shifts from Galactic center to anticenter
  - → **sources extragalactic!**

UHECR flux from Large Scale Structure

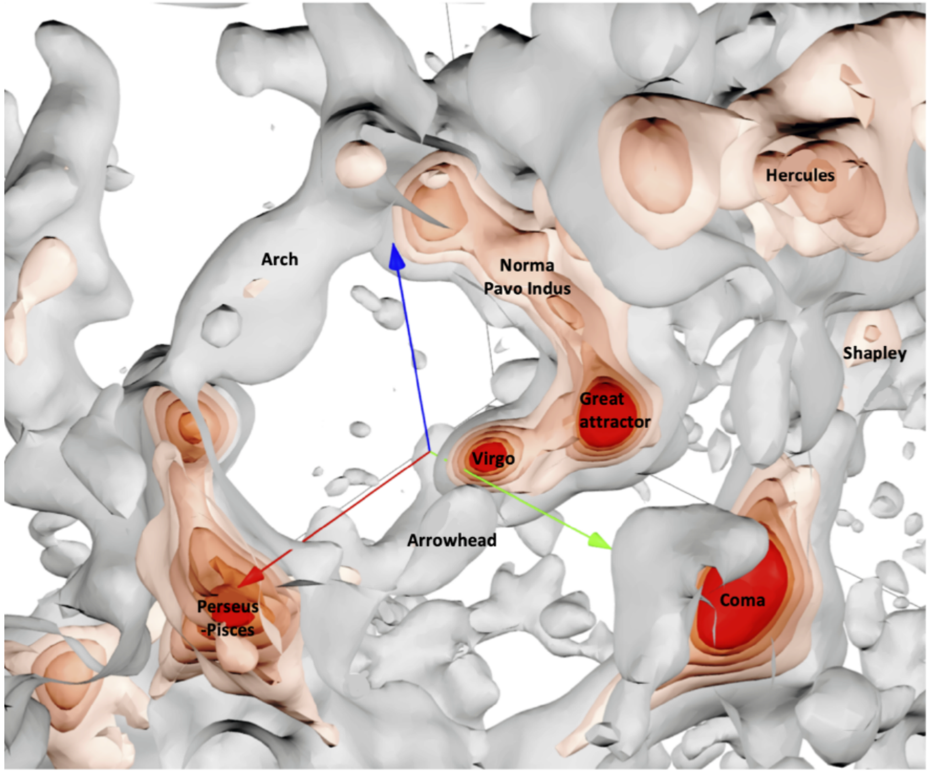

extragalactic matter density

dipole > 8 EeV, >5σ

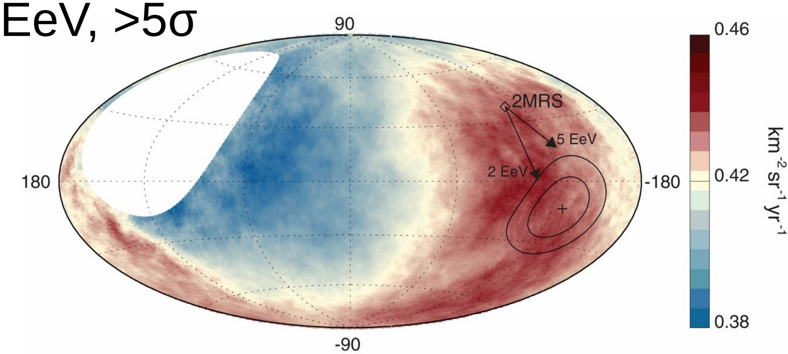

dipole can be explained by extragalactic sources following the **large-scale structure of the universe**

+ deflection by Galactic magnetic field

e.g. Ding, Globus, Farrar ApJL 913 L13 (2021)
Globus, Piran, Hoffman, Carlesi, Pomarede MNRAS 484 (2019)
Allard, Aublin, Baret, Parizot A&A 664 A120 (2022)
...

Bister & Farrar, ApJ 966 71 2024

UHECR flux from Large Scale Structure

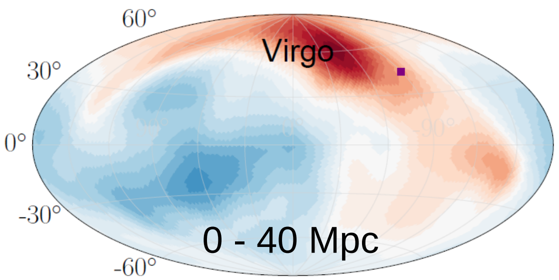

+

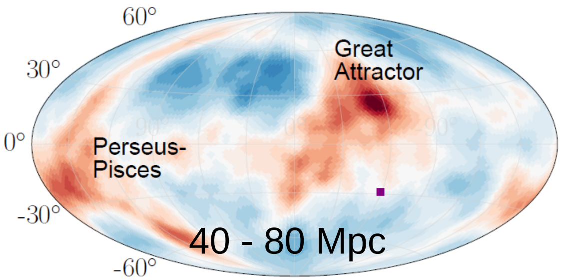

+

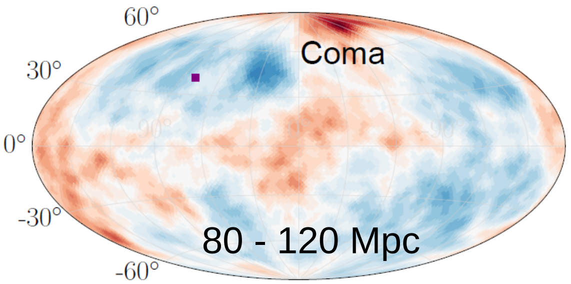

+ ...

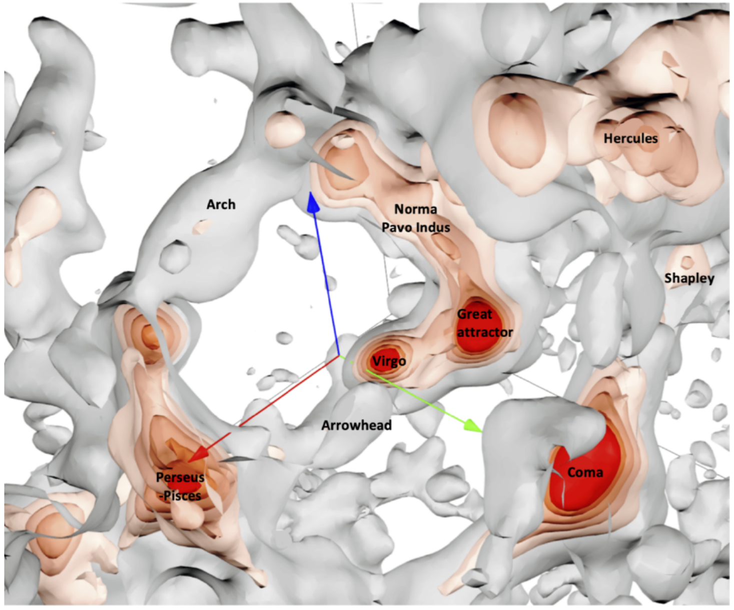

=

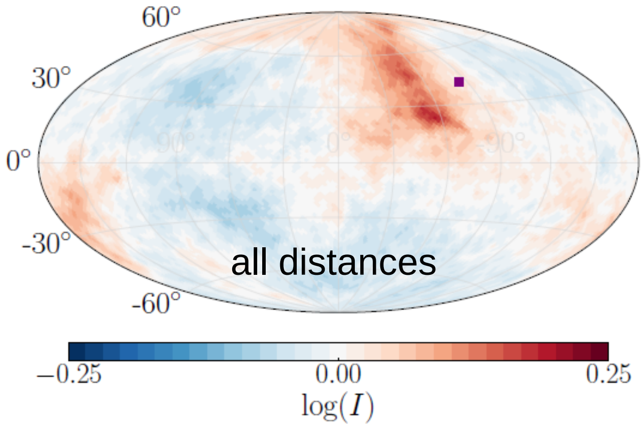

expected flux at the edge of our Galaxy

„illumination“

Bister & Farrar, ApJ 966 71 2024

Measurements at Earth (after Galactic magnetic field)

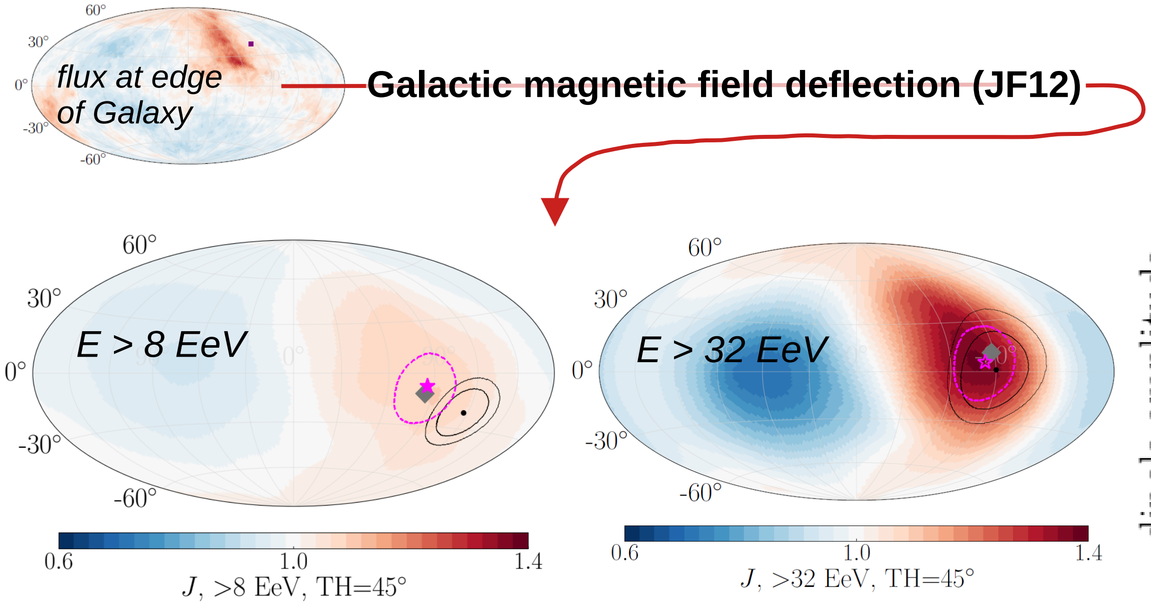

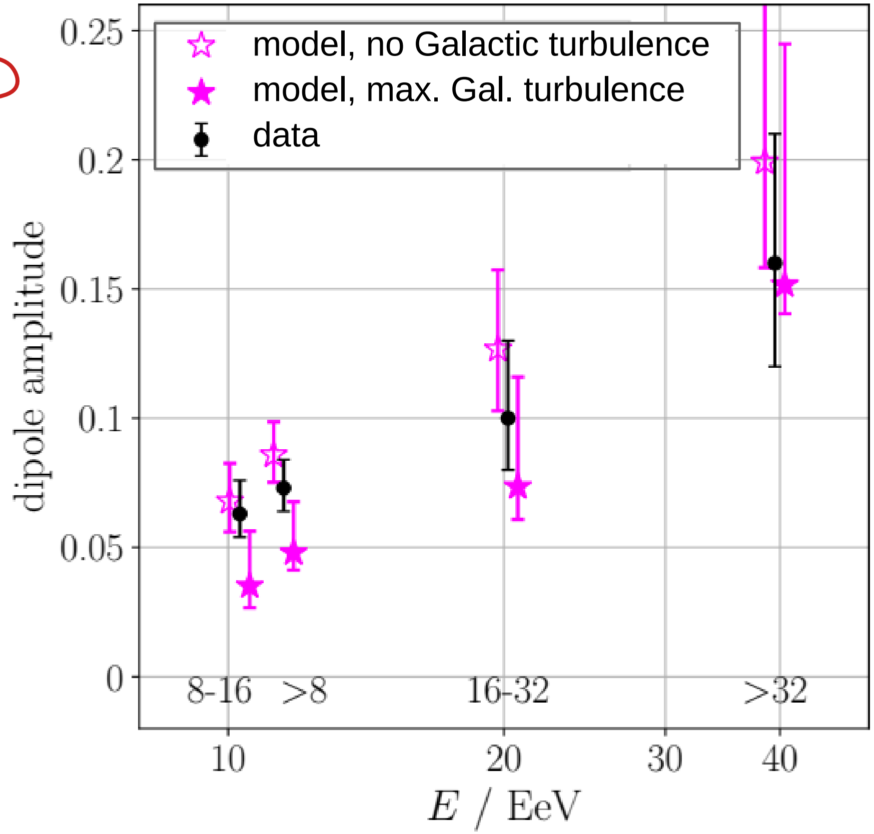

- dipole direction not perfect at lower energy
  → update of GMF model? later
- dipole amplitude + energy evolution ✓

Measurements at Earth (after Galactic magnetic field)

energy spectrum ✔

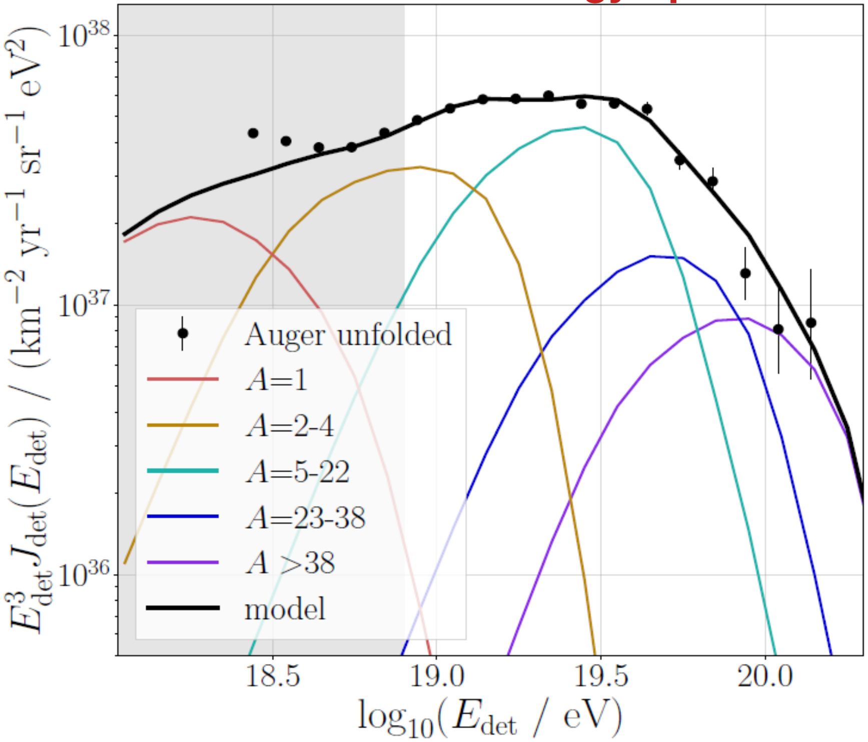

mass composition ✔

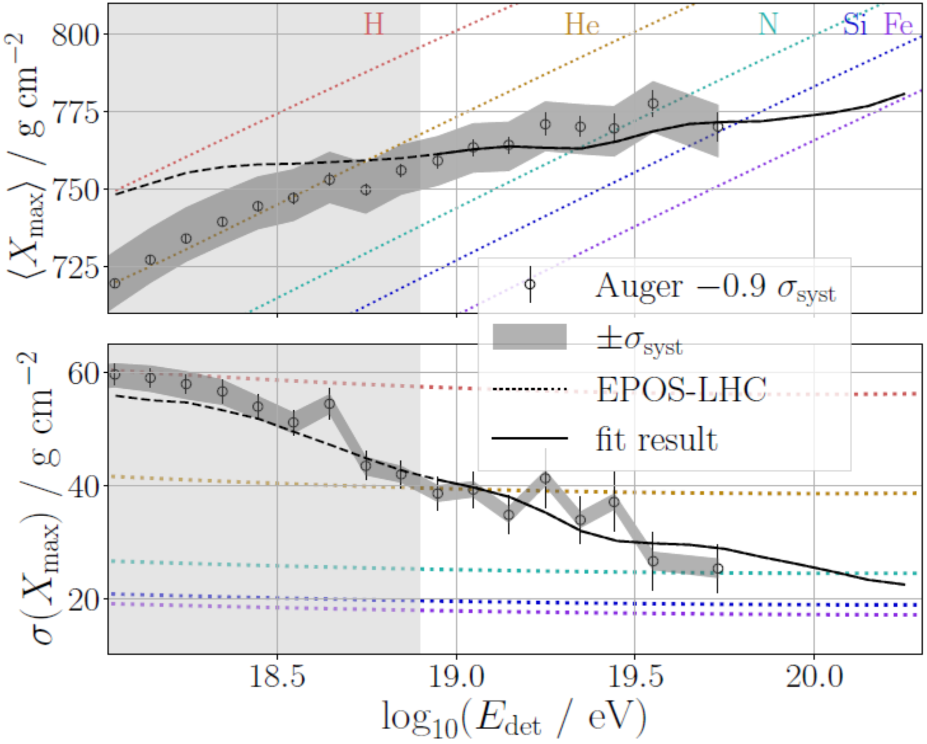

LSS model can describe spectrum, composition and arrival directions. What else can we learn…?

Bias between matter density and UHECR sources

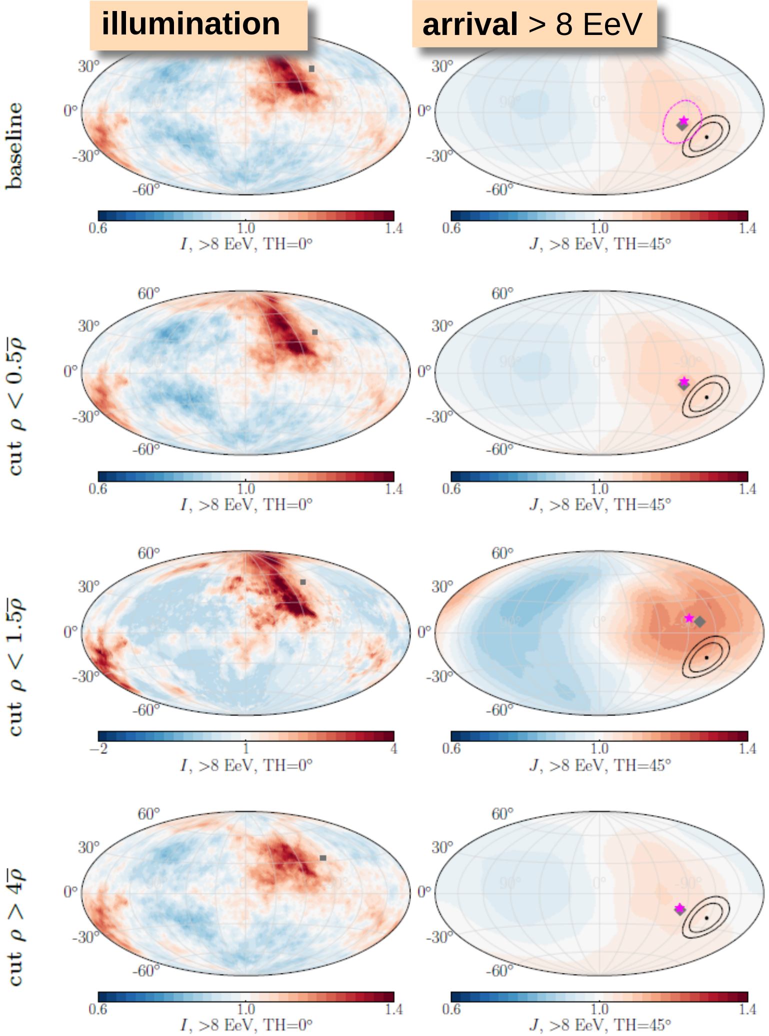

*Is there a **bias** between the UHECR source distribution and the (dark) matter distribution / LSS?*

→ simple test:
cut away densest / least dense regions of LSS

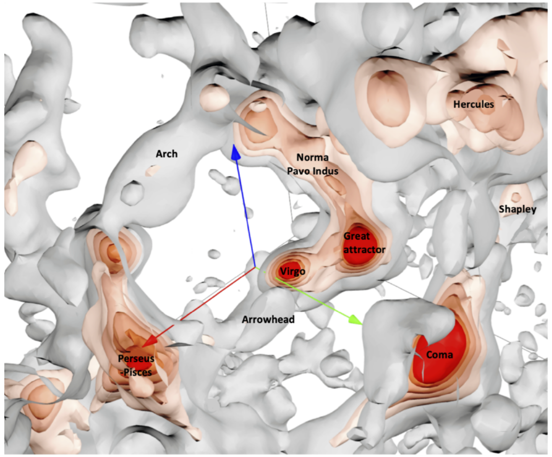

Bister & Farrar, ApJ 966 71 2024

Bias between matter density and UHECR sources

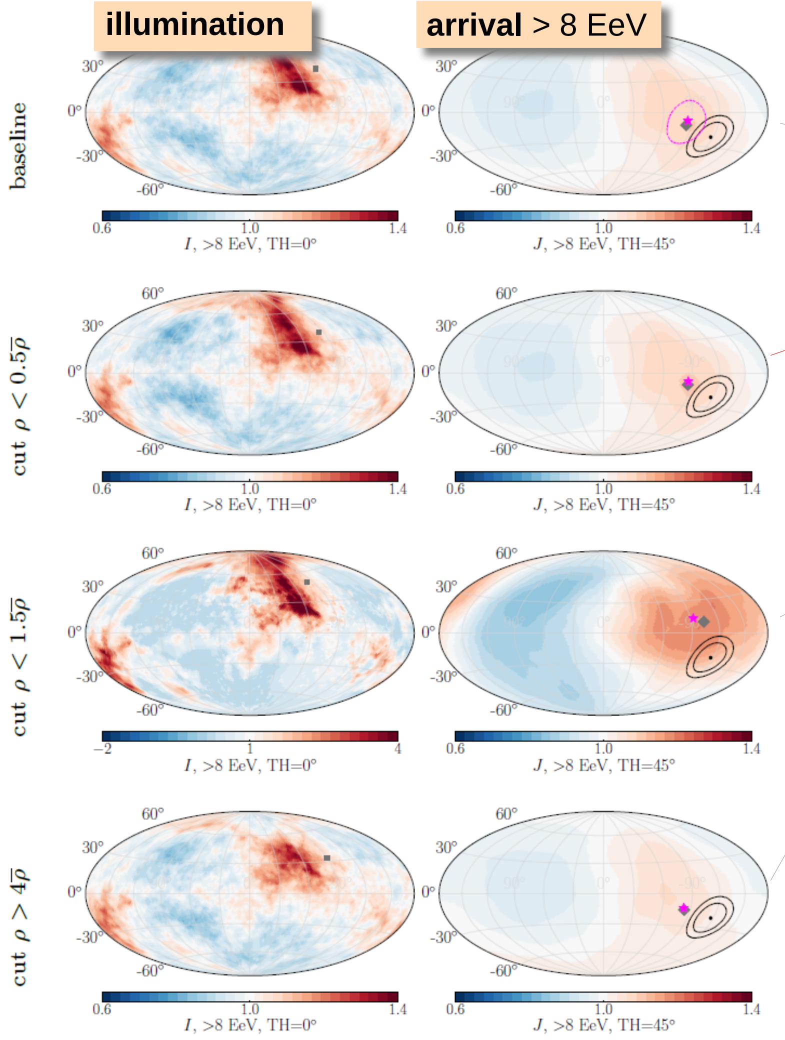

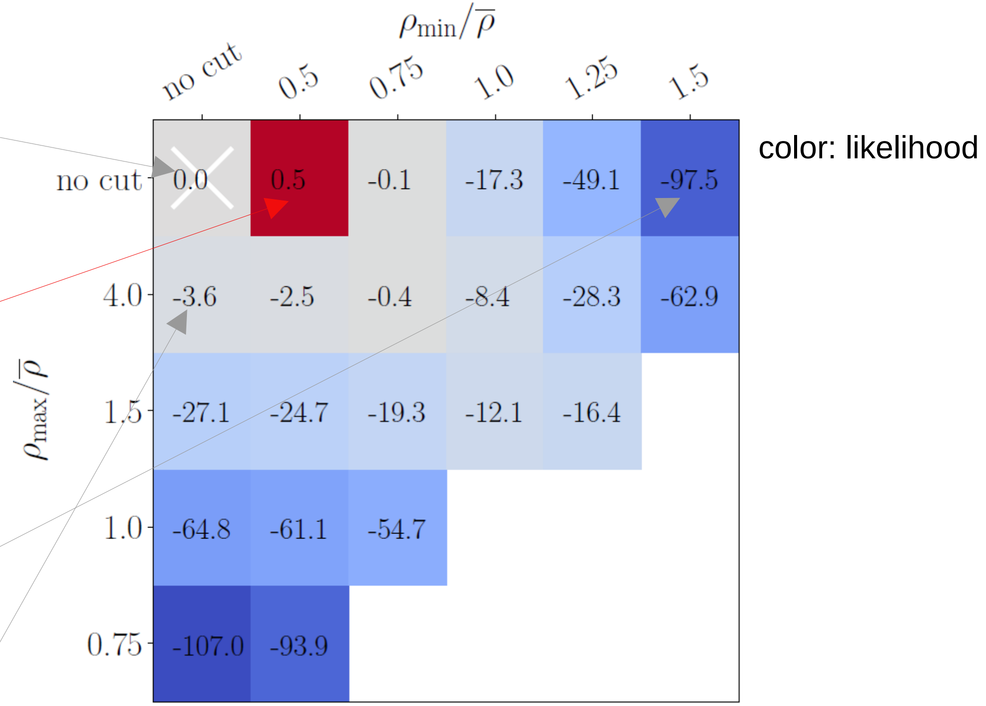

- sources in matter-dense and average regions, no definite conclusion on low-density regions
- **(dark) matter density (almost) unbiased proxy for UHECR source density**

Extragalactic magnetic field effect?

- extragalactic magnetic field „smears out“ arrival directions
- cannot be too strong to not decrease dipole amplitude

$$\delta\theta = 2.9^\circ \frac{B}{\mathrm{nG}} \frac{10\,\mathrm{EV}}{E/Z} \frac{\sqrt{D\ L_c}}{\mathrm{Mpc}}$$

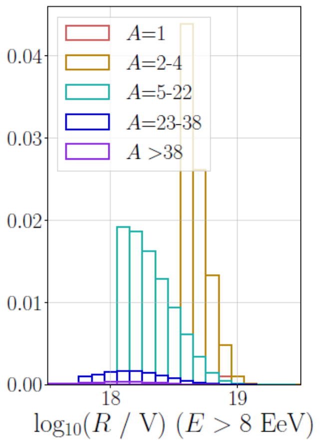

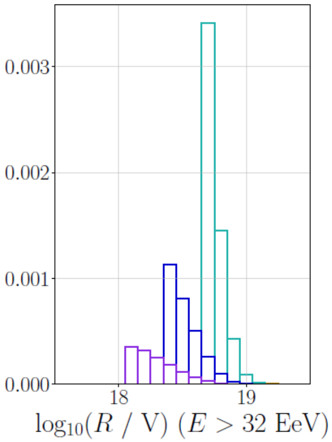

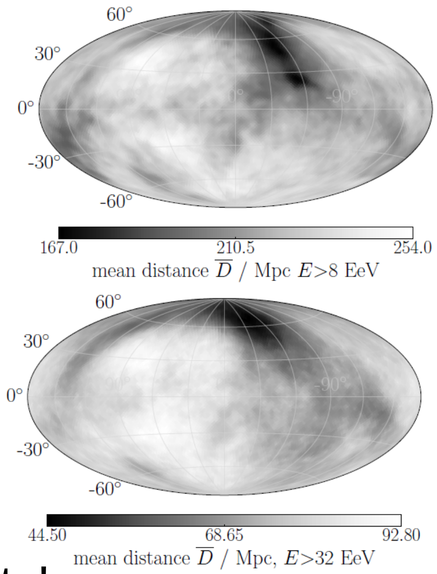

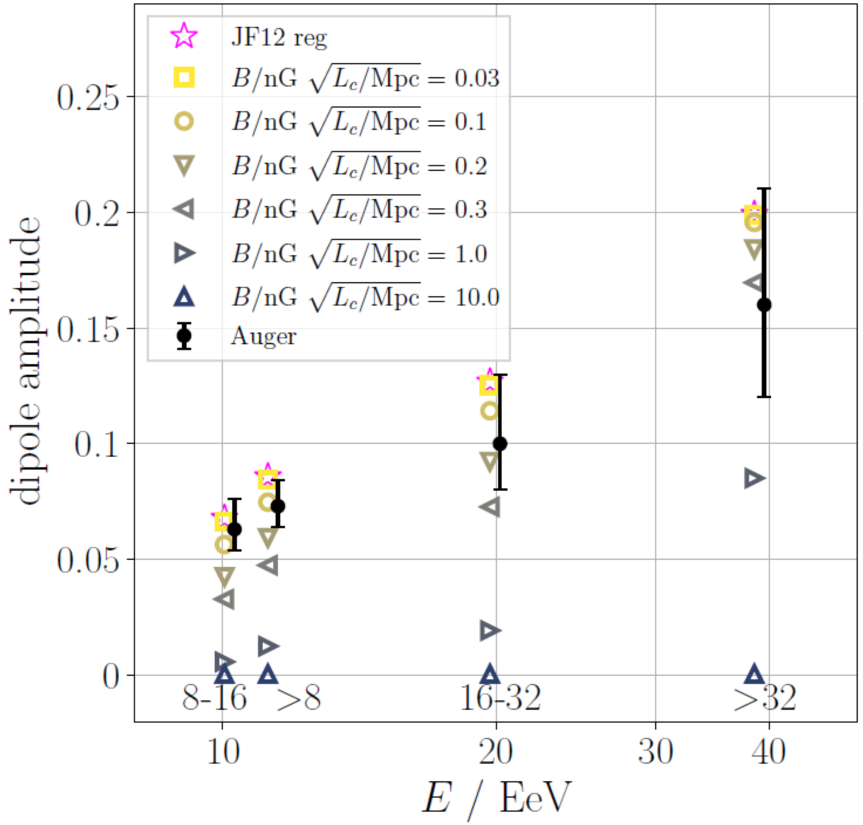

but - opposing effect:
sparser source number density!

Source density and extragalactic magnetic field

extragalactic magnetic field

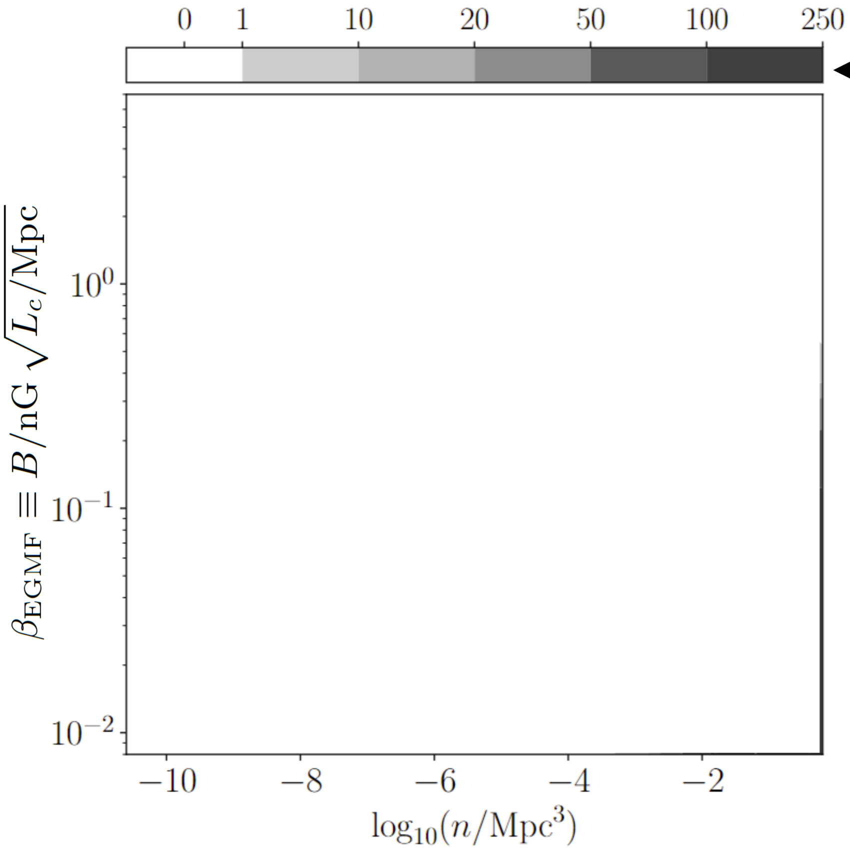

source number density

„How many of 1000 random simulations have a large enough dipole and small enough higher multipole moments?“

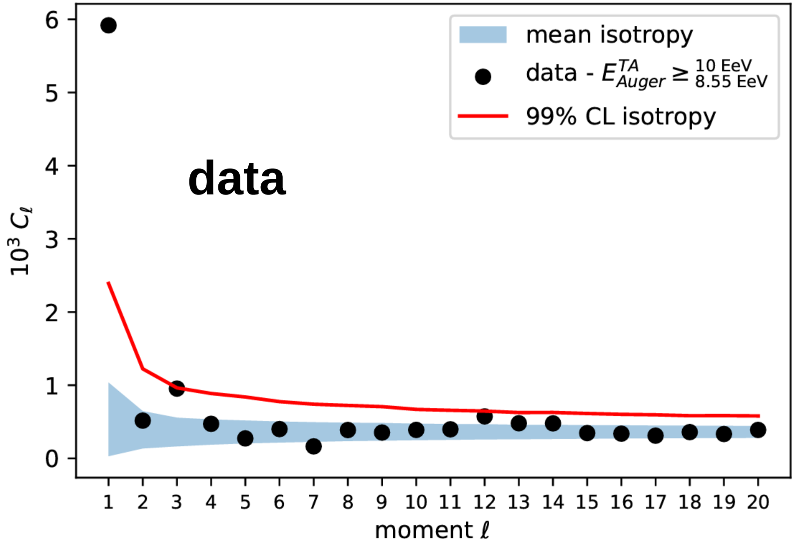

Bister & Farrar, ApJ 966 71 2024

Source density and extragalactic magnetic field

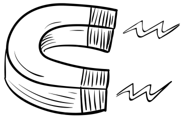

extragalactic magnetic field

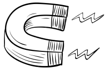

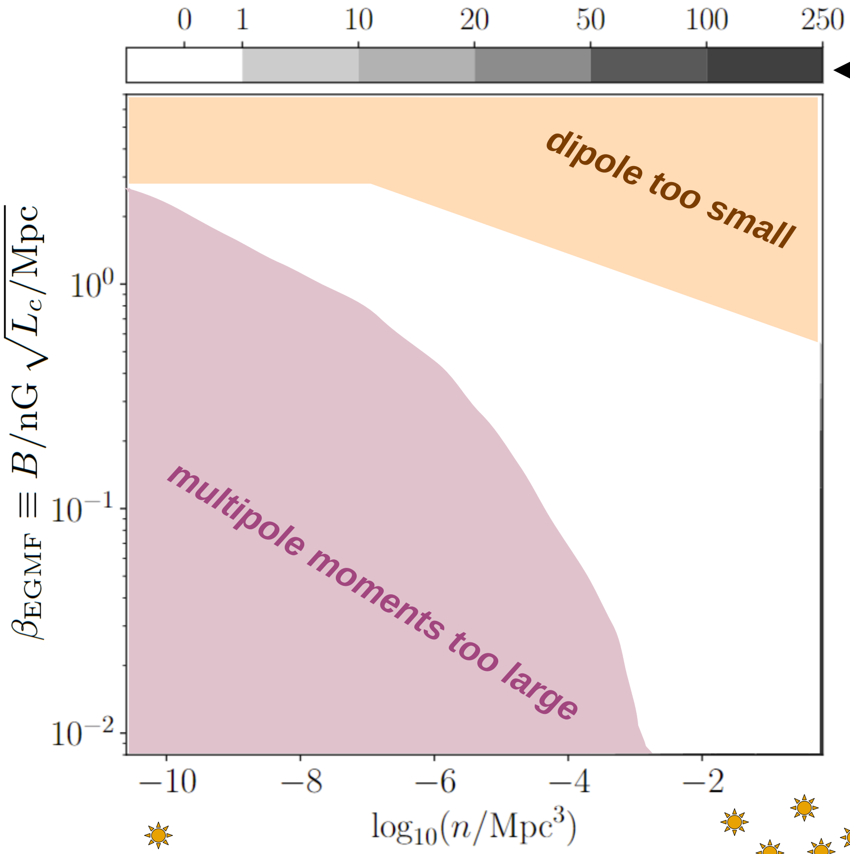

„How many of 1000 random simulations have a large enough dipole and small enough higher multipole moments?“

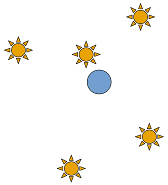

source number density

„cosmic variance“

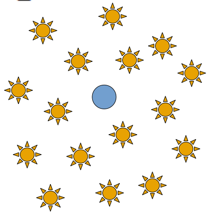

Bister & Farrar, ApJ 966 71 2024

Source density and extragalactic magnetic field

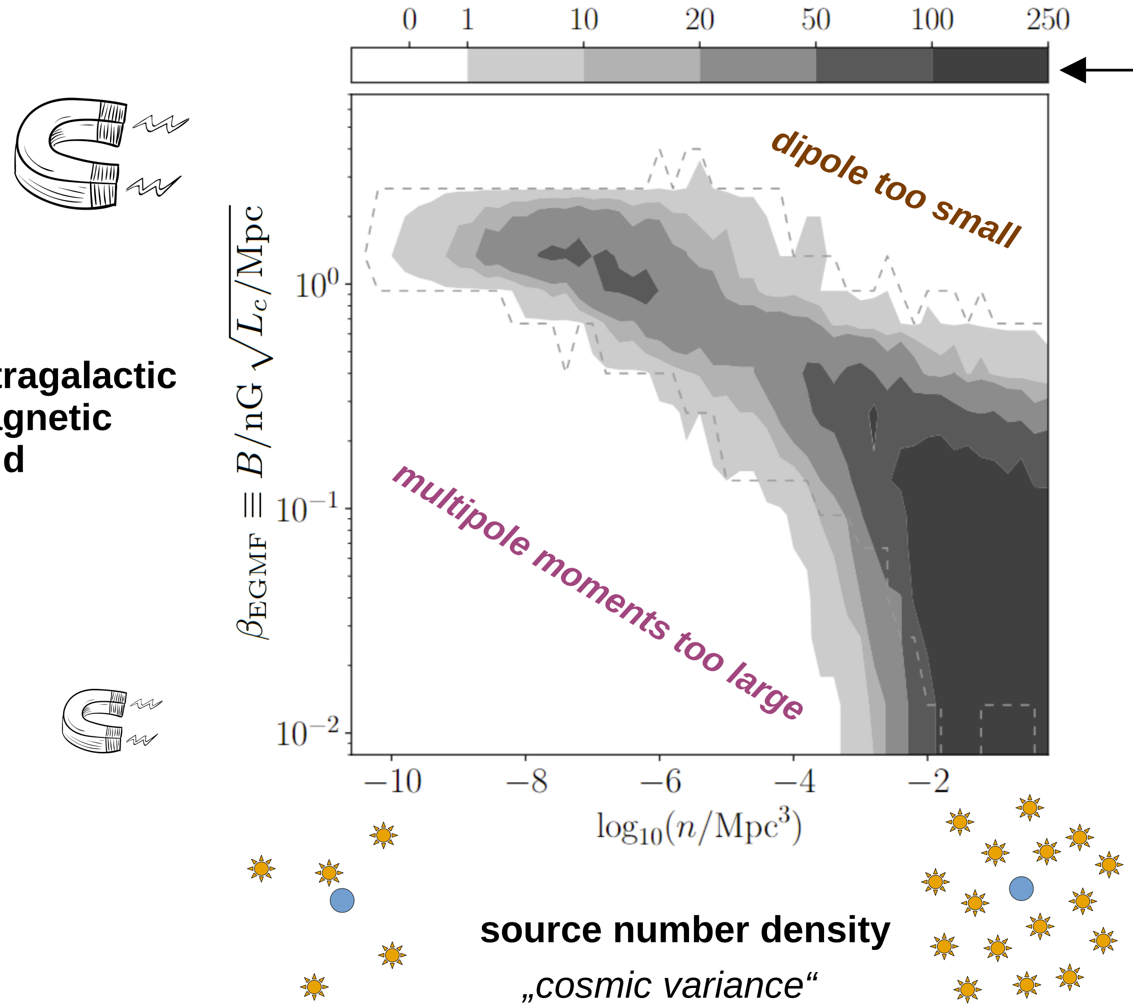

„How many of 1000 random simulations have a large enough dipole and small enough higher multipole moments?“

extragalactic magnetic field

source number density

„cosmic variance“

Source density and extragalactic magnetic field

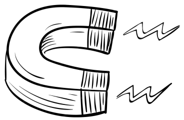

extragalactic magnetic field

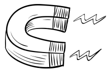

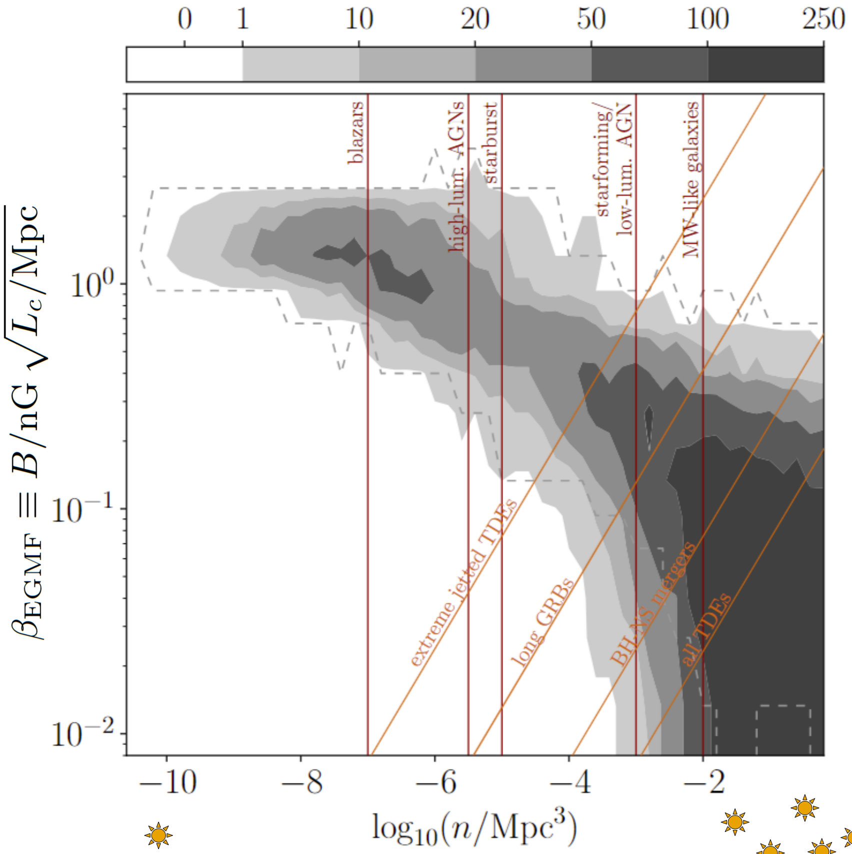

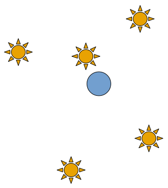

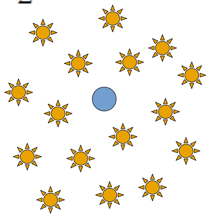

source number density

„cosmic variance“

- **rare sources** (e.g. starbursts) ↔ **strong EGMF**
  - max. 3 nG Mpc$^{1/2}$
- **negligible EGMF** ↔ sources must be **common**, (e.g. Milky-Way-like galaxies)
  - or: **frequent** in case of **transients** like BH-NS mergers, tidal disruption events

Source density and extragalactic magnetic field

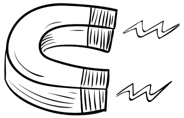

extragalactic magnetic field

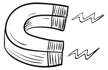

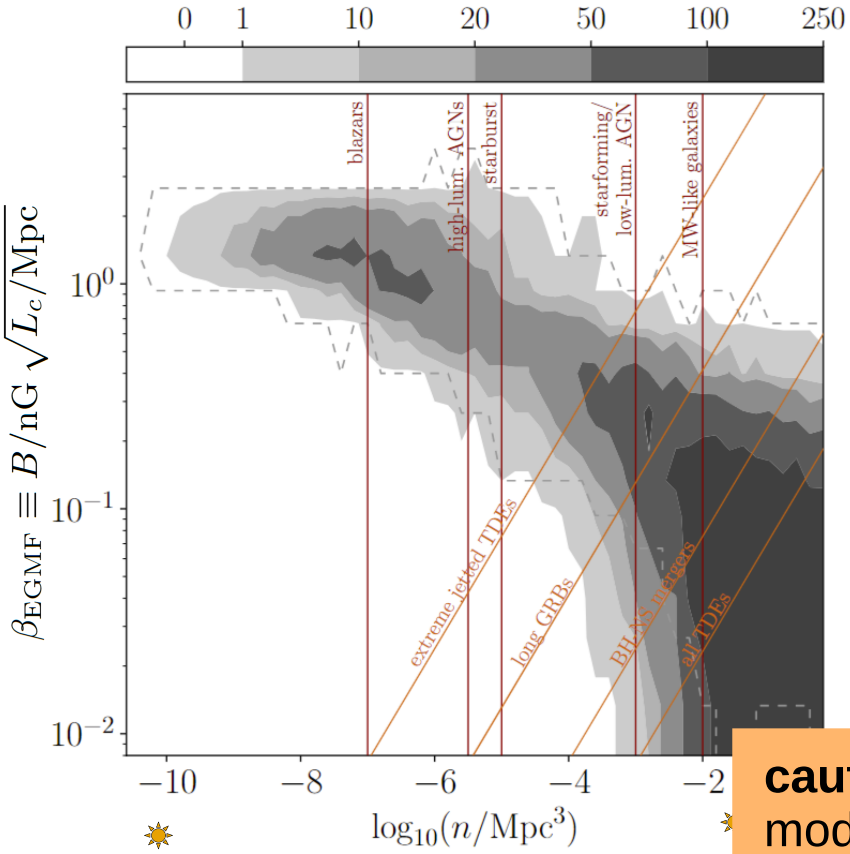

source number density

„cosmic variance“

- **rare sources** (e.g. starbursts) ↔ **strong EGMF**
  - max. 3 nG $\mathrm{Mpc}^{1/2}$
- **negligible EGMF** ↔ sources must be **common**, (e.g. Milky-Way-like galaxies)
  - or: **frequent** in case of **transients**

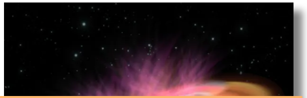

caution: dependencies on coherent GMF model, random GMF part, EGMF simplification, uncertainties on source distribution...

Homogeneous source distribution?

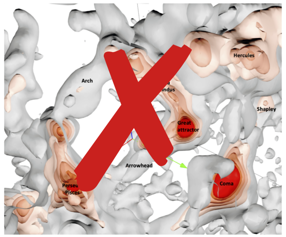

extragalactic magnetic field

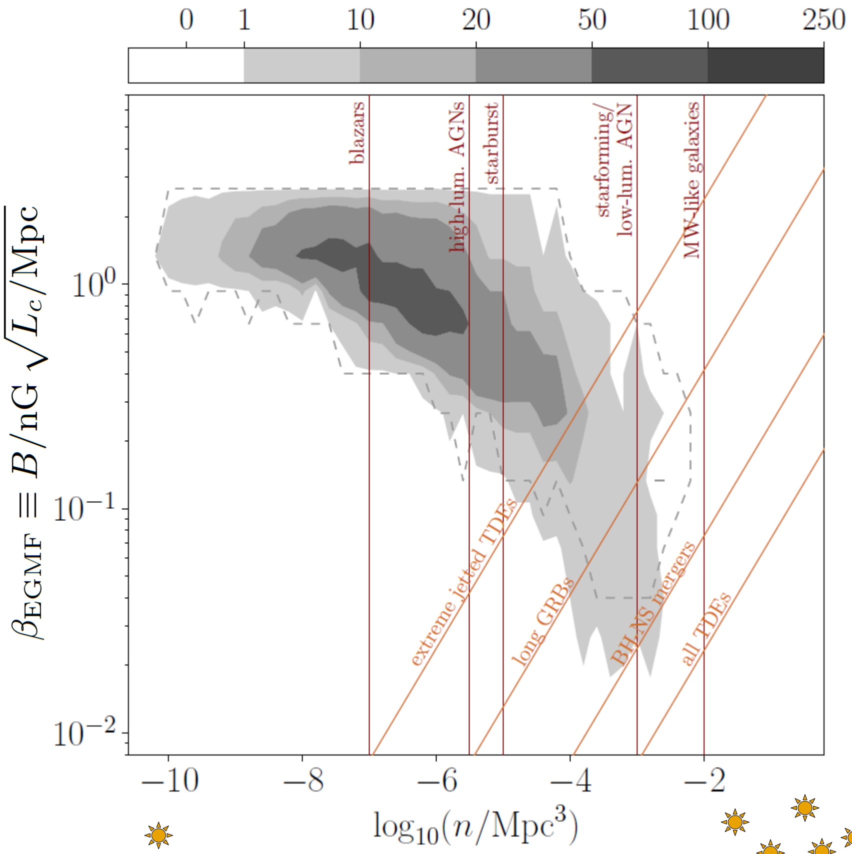

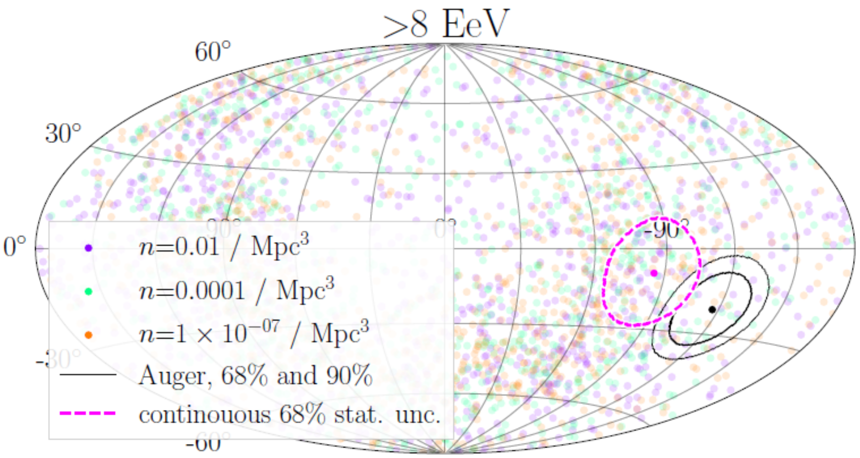

- homogeneous distribution less likely, only for rare sources and considerable EGMF
- dipole direction not predictable

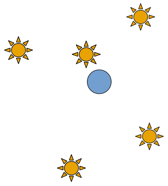

source number density

„cosmic variance“

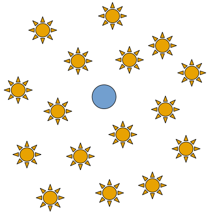

New models for the Galactic magnetic field

source distribution

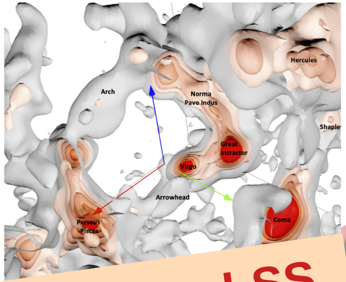

following LSS

injection

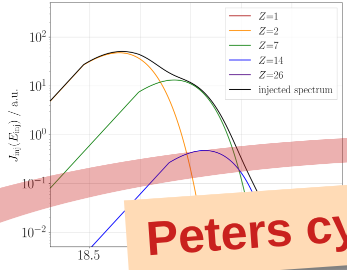

Peters cycle

propagation through extragalactic space

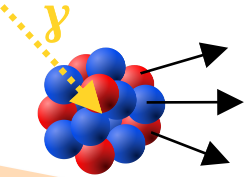

SimProp SIRENTE

CRPropa

1-dimensional

extragalactic magnetic fields

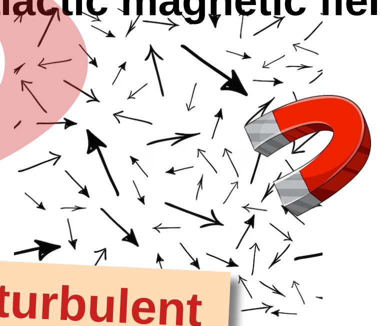

turbulent

Galactic magnetic fields

new UF23 models

compare to data

- energy spectrum
- mass composition
- arrival directions
- (multimessenger)

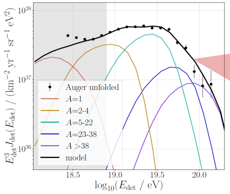

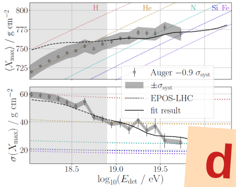

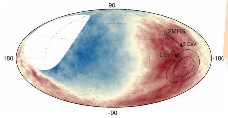

dipole E>8 EeV

Dipole directions

predict **dipole direction for 8 new GMF models** (+Planck random field):

- models quite similar → cannot reject any model
  → good news: GMF uncertainty does not obstruct conclusions on sources 🙂
- random field part has minor influence on dipole direction
- **biggest uncertainty: from cosmic variance**

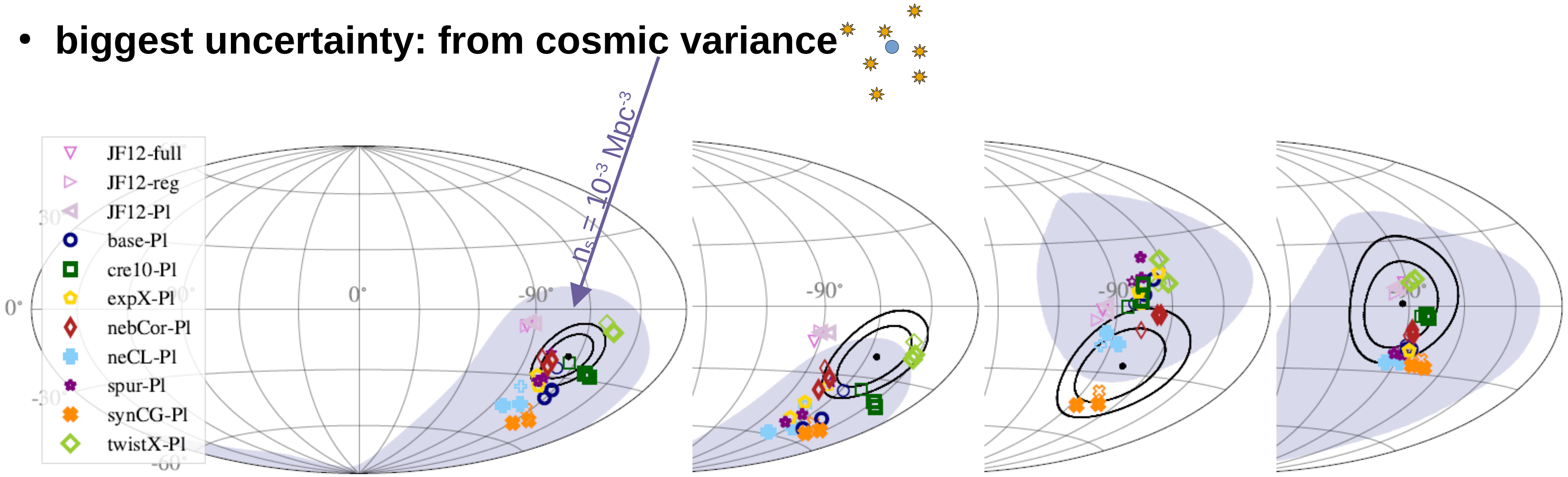

(a) energy > 8 EeV (b) (8 – 16) EeV (c) (16 – 32) EeV (d) > 32 EeV

Dipole & Quadrupole amplitudes

dipole & quadrupole amplitudes:

- cosmic variance again dominates over differences between models
- quadrupole amplitude of all UF23 model comparable to JF12 + Planck

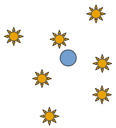

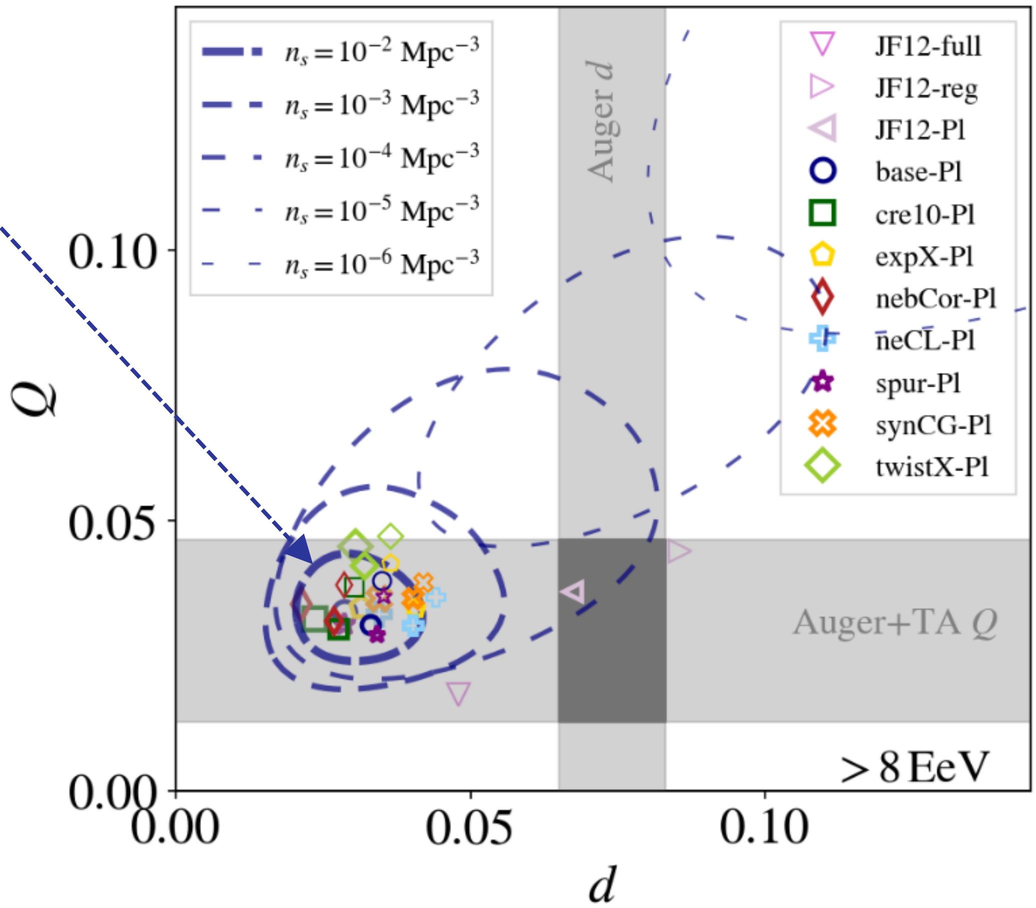

Dipole & Quadrupole amplitudes

dipole & quadrupole amplitudes:

- cosmic variance again dominates over differences between models
- quadrupole amplitude of all UF23 model comparable to JF12 + Planck
- but: **dipole amplitude significantly smaller!**
  - → now need approximately 10^{-3} Mpc^{-3} < n < 10^{-5} Mpc^{-3} for compatibility
  - → continuous model incompatible!

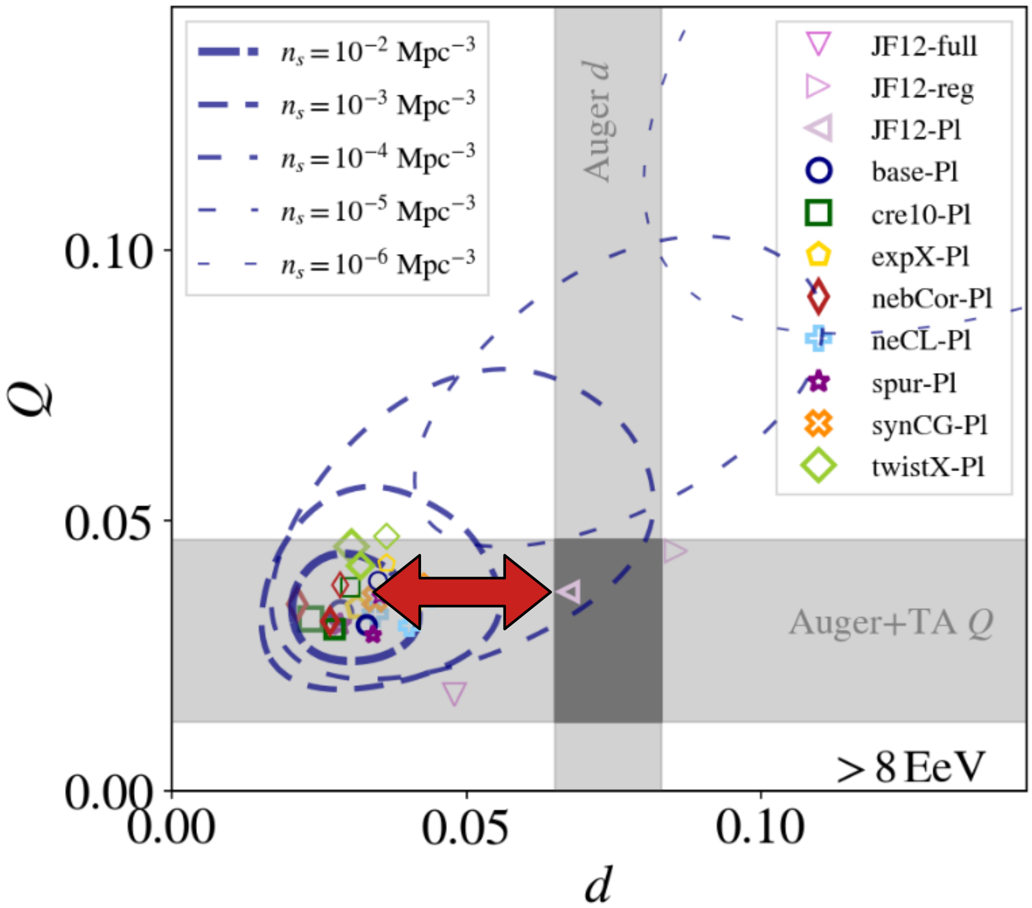

Why is the dipole amplitude so small with UF23?

- highest flux illumination is **demagnified by *all* UF23 models**, different to JF12

magnification = flux with GMF divided by flux without GMF, from every direction

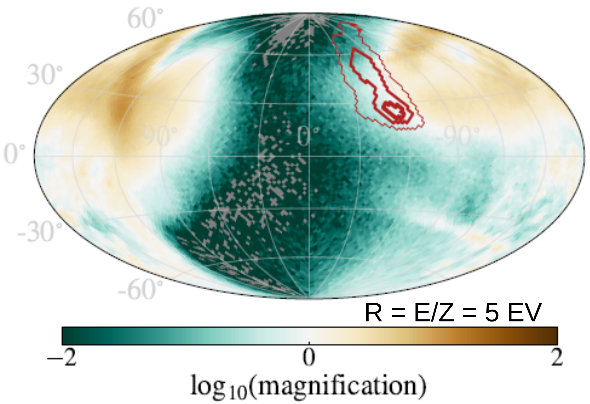

JF12 + Planck

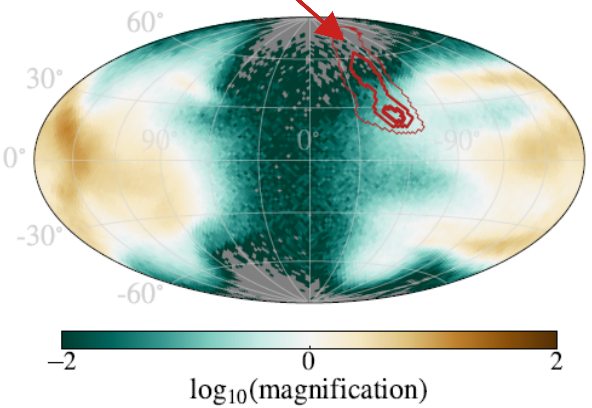

UF23 base + Planck

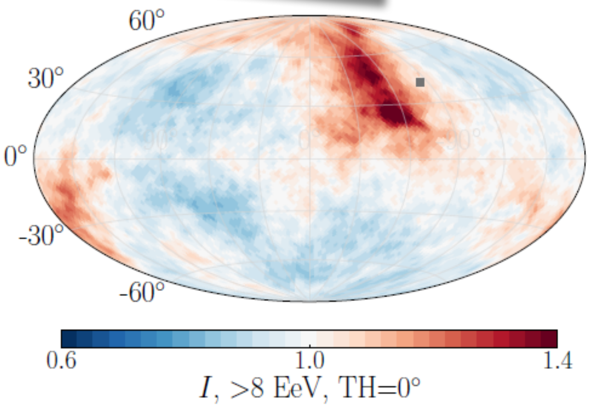

illumination E>8 EeV

- **magnification has huge influence on dipole amplitude!**
  - due to uncertainties on LSS model + random magnetic field model + EGMF:
    → source density etc. with large uncertainties
  - future: sensitivity to probe LSS model, GMF...

Bister, Farrar, Unger in prep.

Magnification maps for different rigidities

consequence of demagnification in UF23 models:

- **many source candidates in central demagnification area**
- night not see many CRs from them, at least not with rigidity R = E/Z < 5 EV

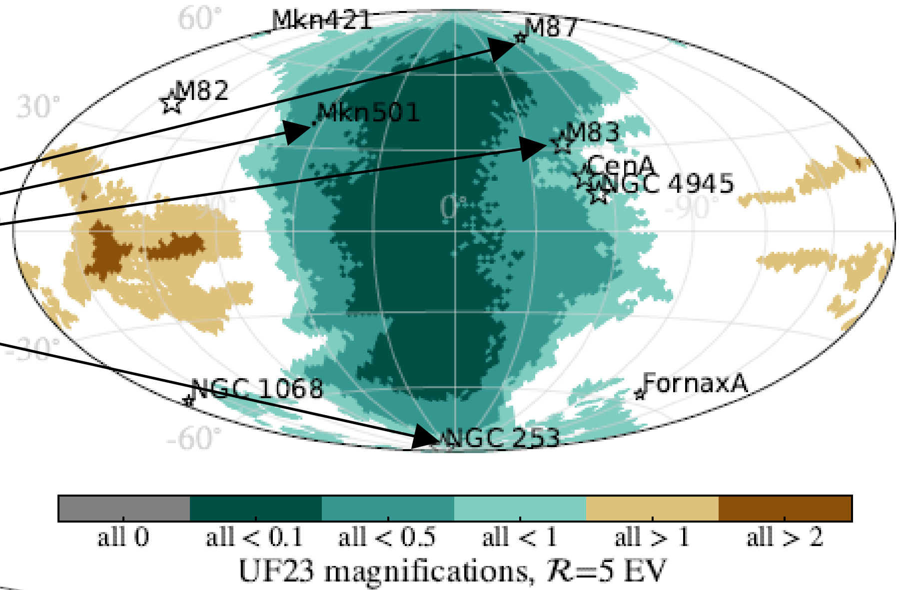

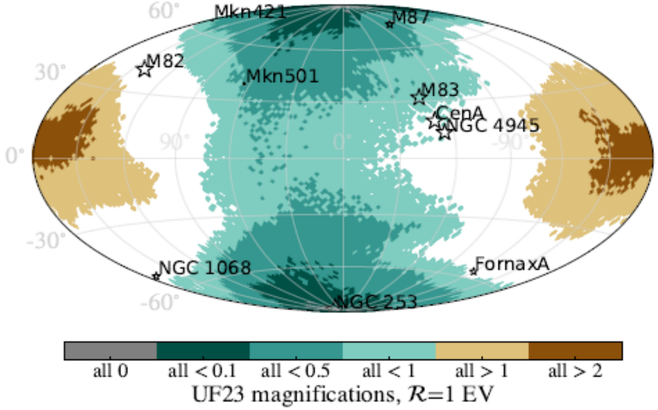

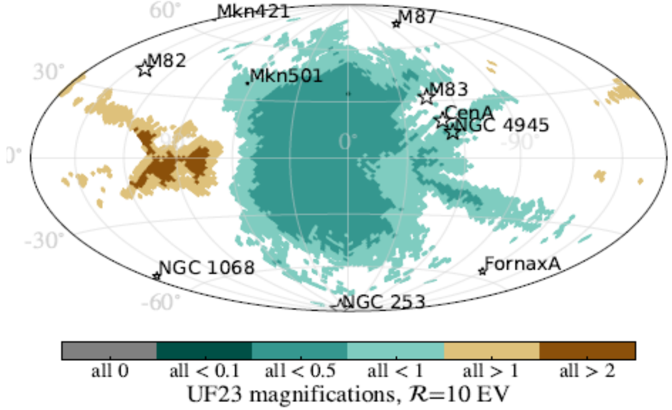

Dipolar illumination

replace the illumination by dipole component:

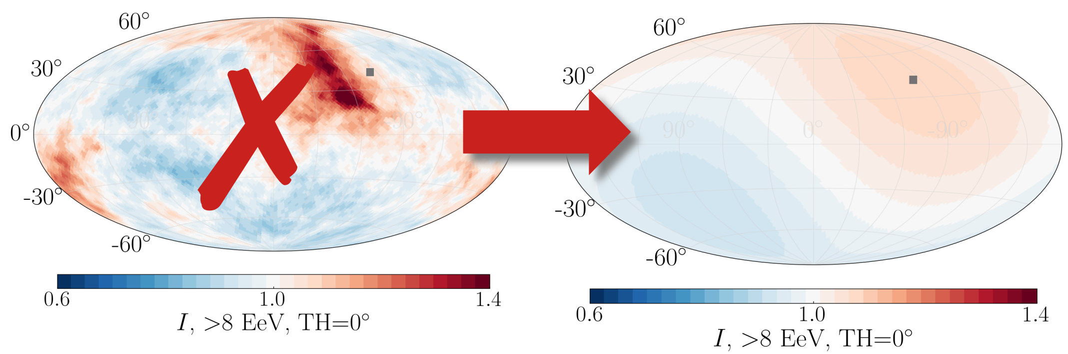

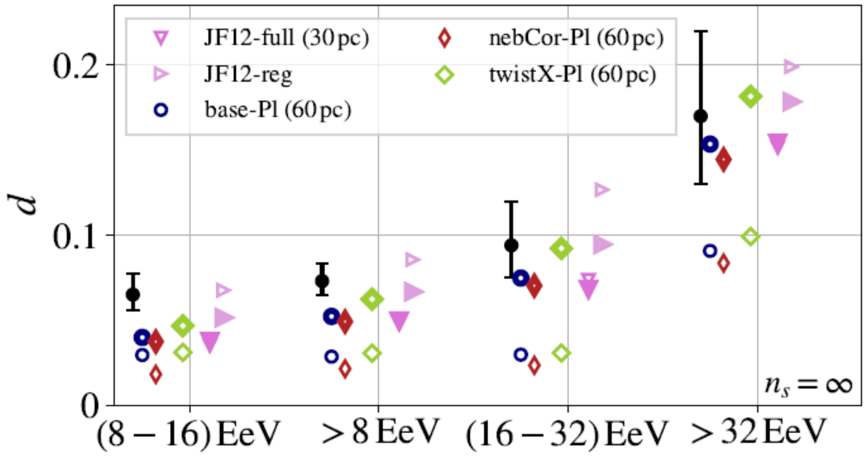

- consequence of sensitive interplay between illumination & magnification
  - **quite different predictions of amplitude (factor 2) & direction (by 20°-60°)**

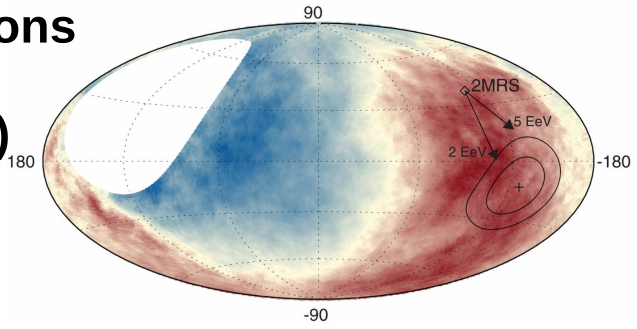

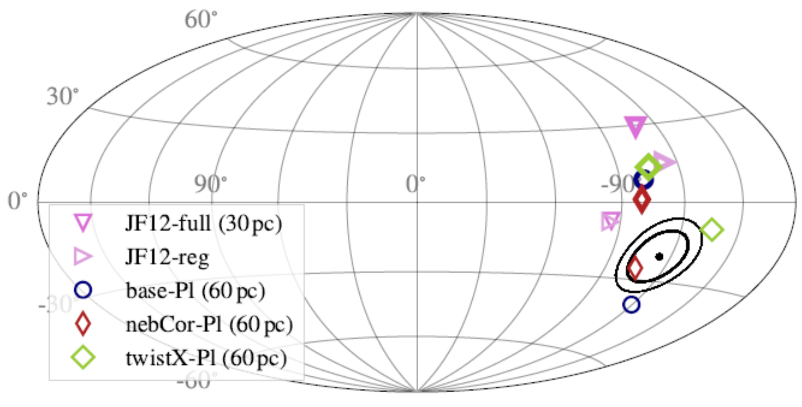

(a) energy > 8 EeV

TB for the Pierre Auger Collaboration, PoS ICRC 2023
The Pierre Auger Collaboration JCAP01(2024)022

Higher energies - smaller-scale anisotropies

source distribution

homogeneous + catalog

injection

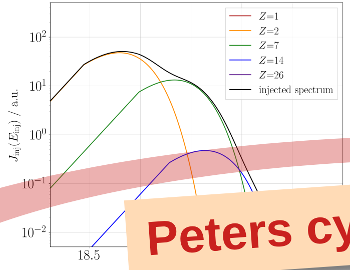

Peters cycle

propagation through extragalactic space

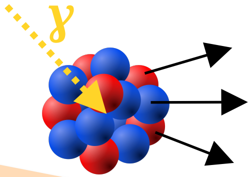

SimProp SIRENTE

CRPropa

1-dimensional

extragalactic magnetic fields

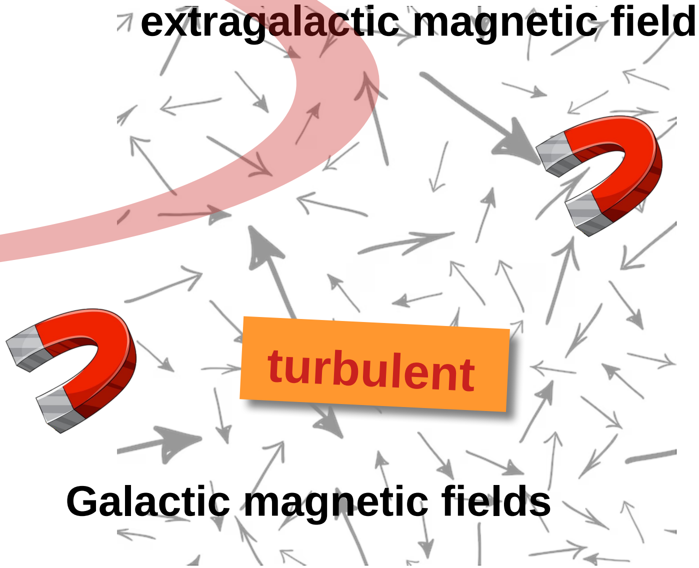

turbulent

Galactic magnetic fields

compare to data

- energy spectrum
- mass composition
- arrival directions
- (multimessenger)

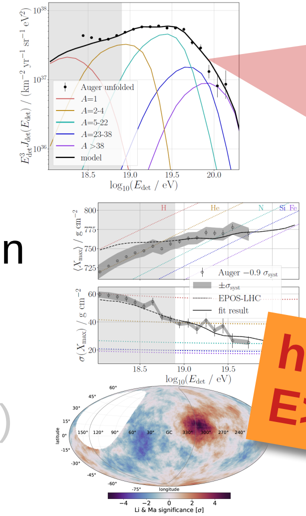

higher energies E>20 EeV

Small-scale anisotropies

- **blind search** over 1° pixels
- 2 scan parameters:
  - energy threshold
    $32\ \mathrm{EeV} \leq E_{th} \leq 80\ \mathrm{EeV}$
  - circular tophat window
    $1° \leq \psi \leq 30°$

local Li-Ma significance: 5.4σ
post-trial **p=3%**

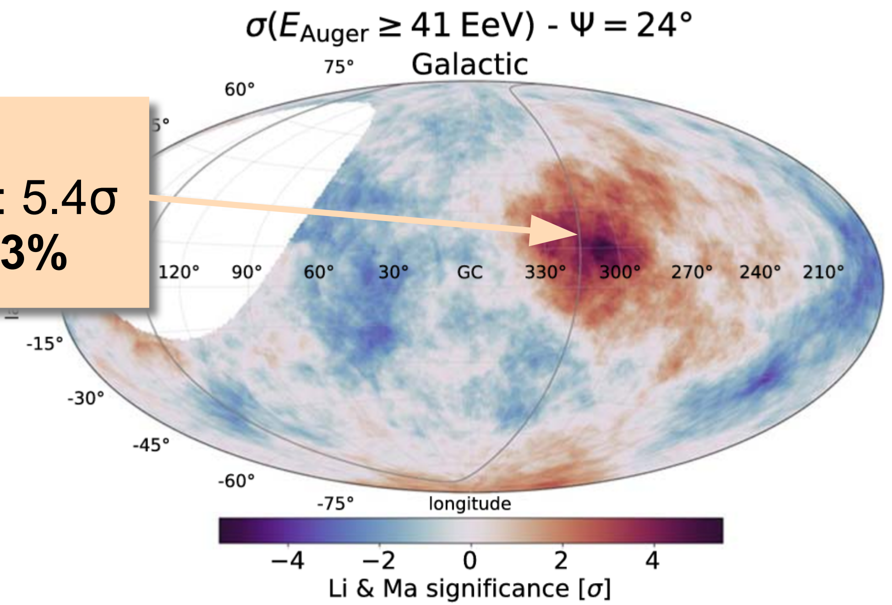

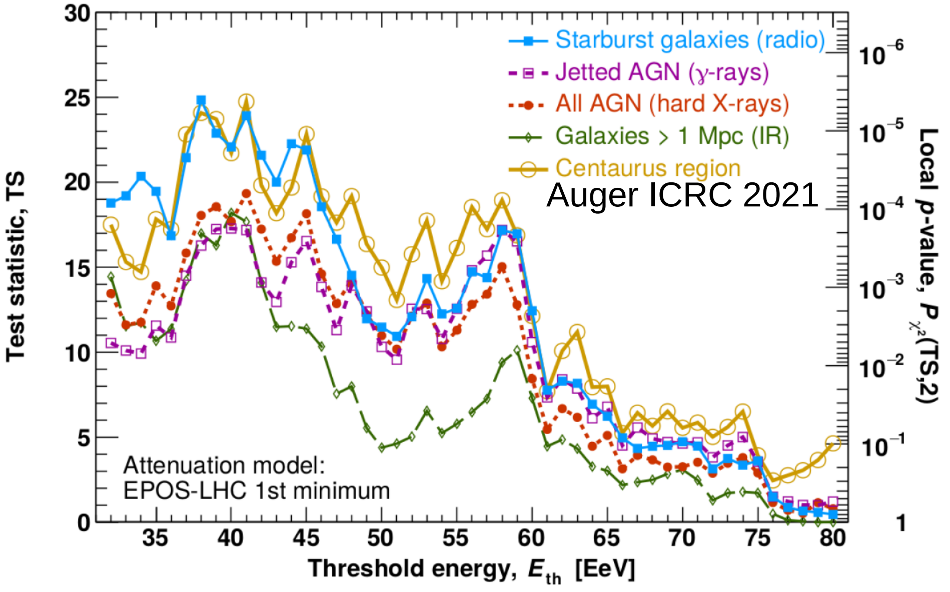

- large trial factor due to whole-sky scan
  → comparison to source candidates
- **currently 4.2σ correlation with catalog of starburst galaxies, 3.3σ with ɣ-AGNs, 4.0σ with Centaurus A**

Model for higher energies

- based on correlations of arrival directions with nearby candidates (SBGs, Centaurus A, ɣ-AGNs)
- model: homogeneous background sources + nearby candidates

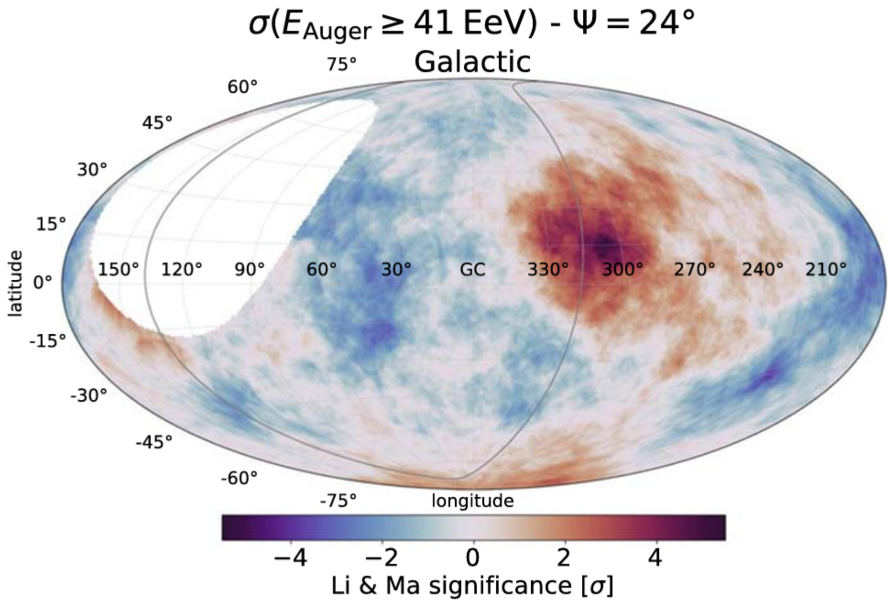

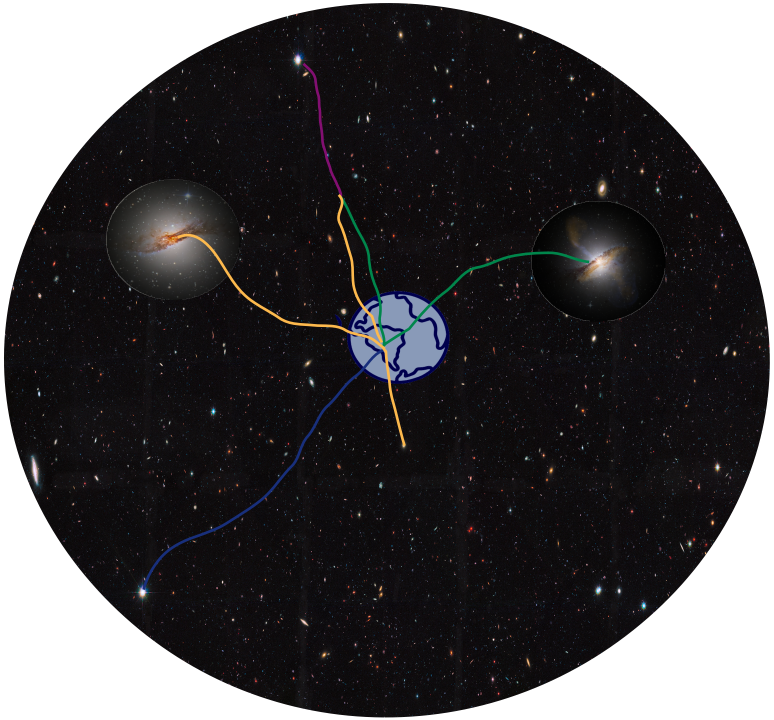

- **fit to energy spectrum, shower depth distributions, arrival directions in energy bins**
- instead of magnetic field models: **rigidity-dependent blurring** $\delta = \frac{\delta_0}{R/10\ \mathrm{EV}}$

R=E/Z

Modeled arrival directions

- based on correlations of arrival directions with nearby candidates (SBGs, Centaurus A, ɣ-AGNs)
- model: homogeneous background sources + nearby candidates

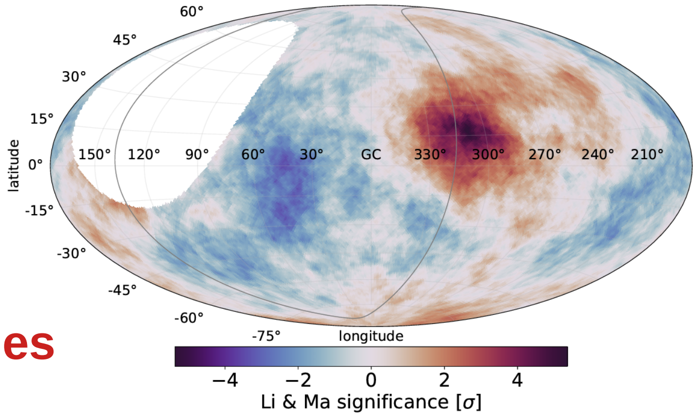

ɣ-AGNs | Centaurus A | Starburst Galaxies

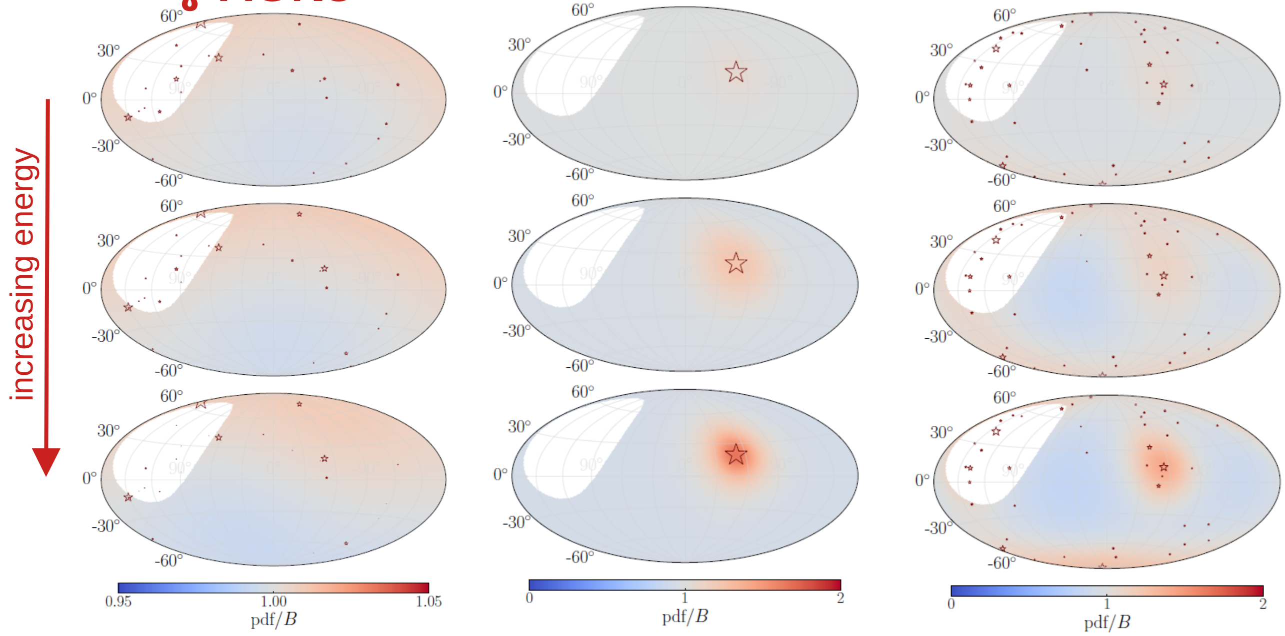

TB for the Pierre Auger Collaboration, PoS ICRC 2023
The Pierre Auger Collaboration JCAP01(2024)022

Modeled arrival directions

- based on correlations of arrival directions with nearby candidates (SBGs, Centaurus A, γ-AGNs)
- model: homogeneous background sources + nearby candidates

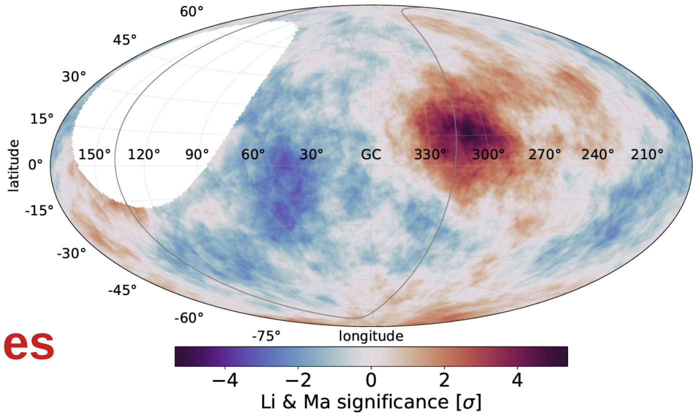

γ-AGNs | Centaurus A | Starburst Galaxies

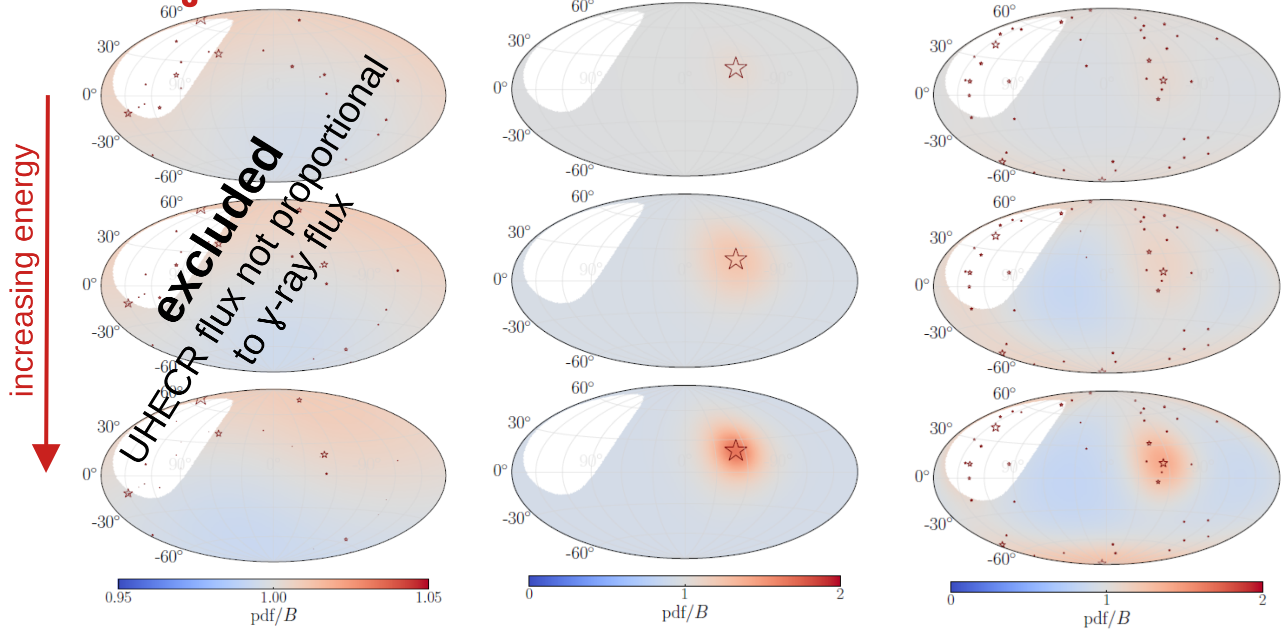

Modeled arrival directions

- based on correlations of arrival directions with nearby candidates (SBGs, Centaurus A, γ-AGNs)
- model: homogeneous background sources + nearby candidates

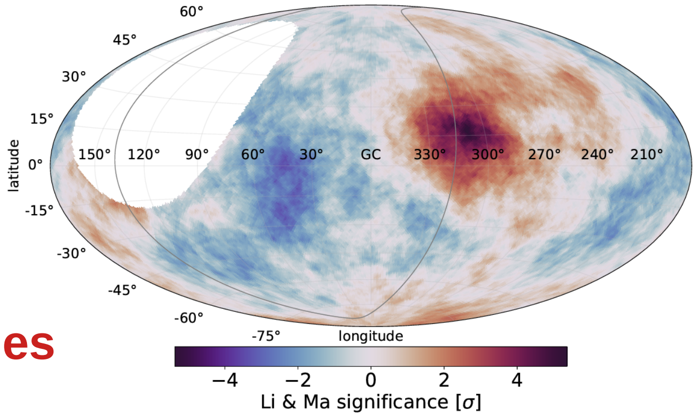

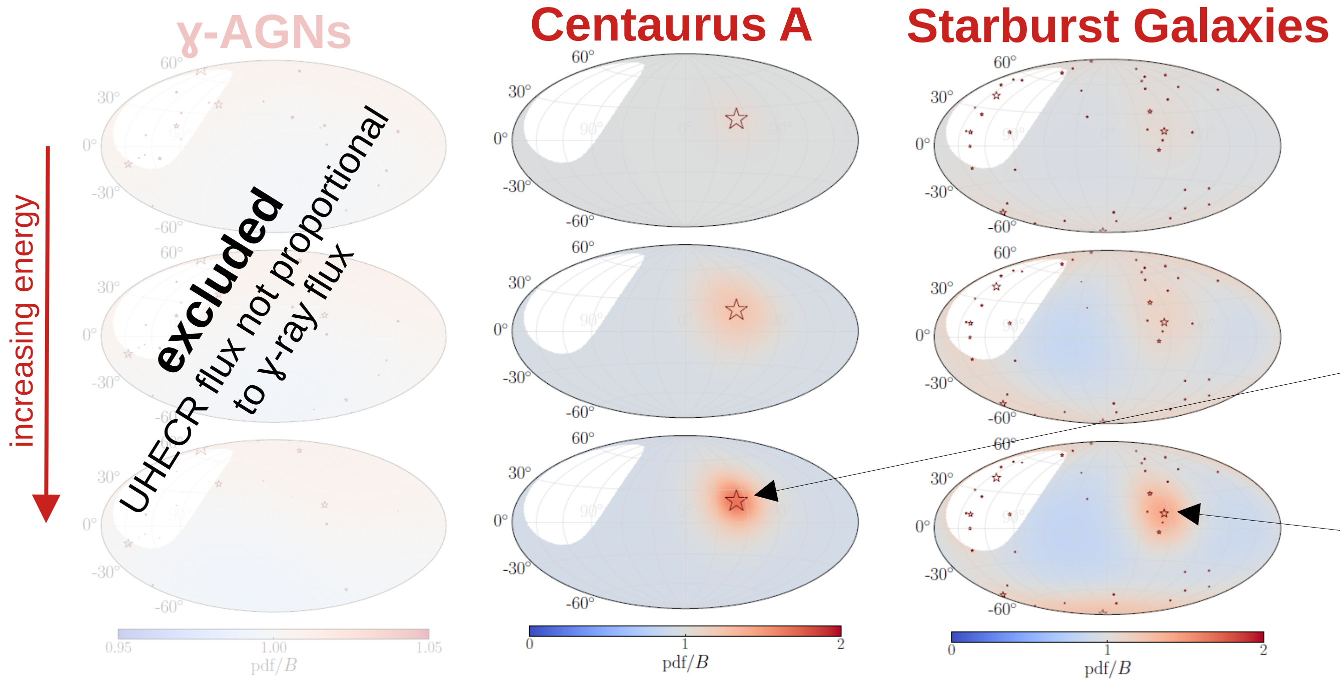

- **starburst galaxy model favored with 4.5σ significance over homogeneous model!**
- mostly due to Centaurus A / NGC 4945 region

Model predictions

- **best-fit:** hard injection spectrum dN/dE ~ E^{-1}, nitrogen-dominated, 20° magnetic field blurring for proton with 10 EeV
- signal fraction ~20% from SBGs, 3% from Centaurus region (at 40 EeV, increases with E)
  - independent of evolution & systematic effects

dashed line = catalog contribution

Centaurus A

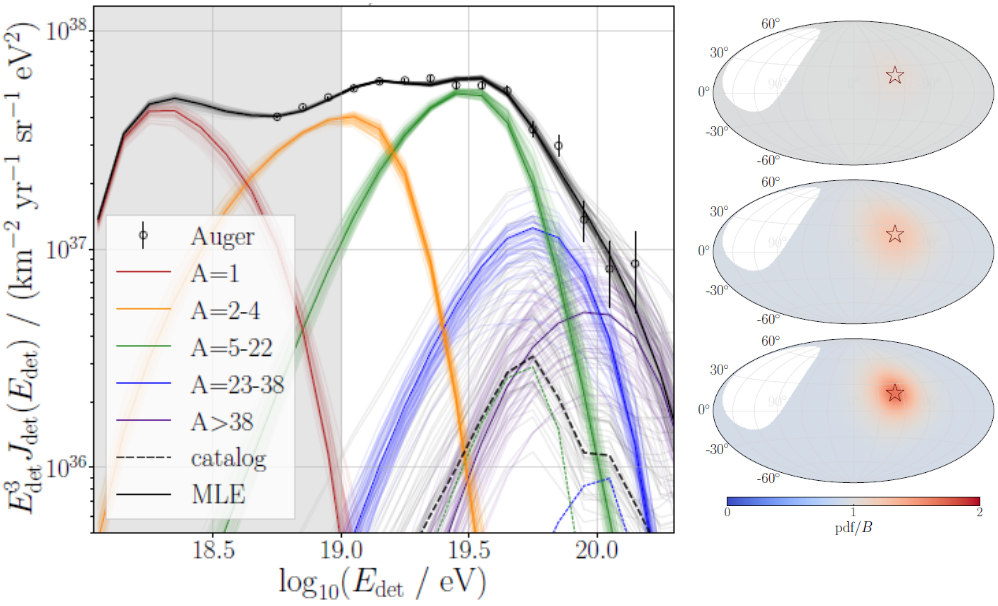

Starburst Galaxies

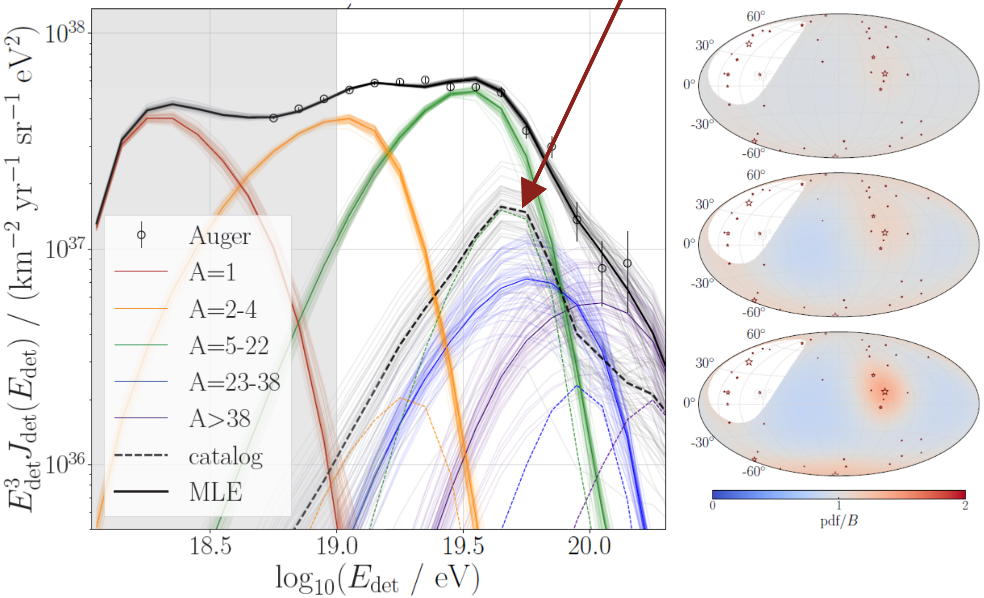

Conclusions

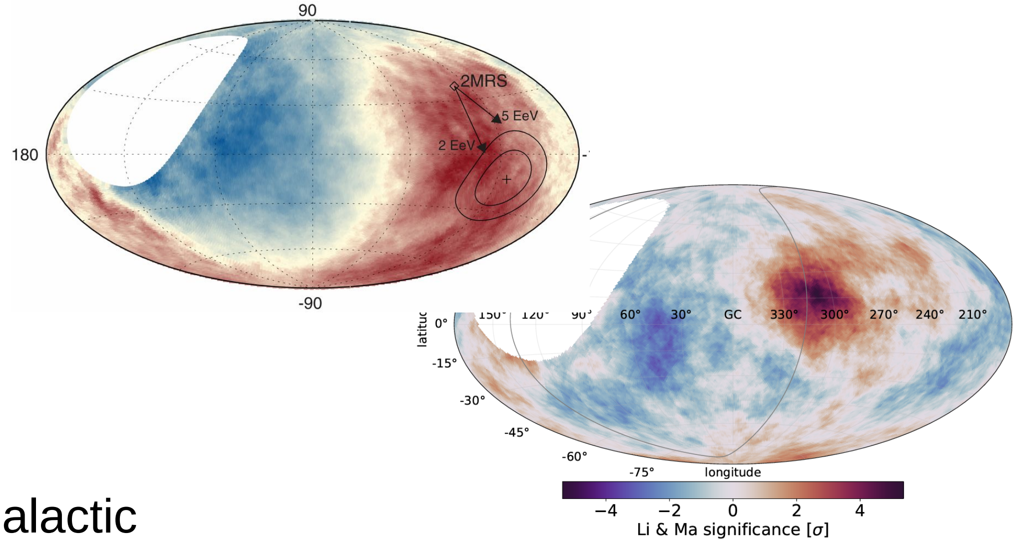

- progress in search for UHECR sources
- need careful modeling of source distribution, propagation, magnetic fields...

➔ **> 8 EeV: sources most likely follow large-scale structure**
  - can infer information on Galactic & extragalactic magnetic fields & source number density

➔ **> 40 EeV: individual source candidates describe data**
  - like starburst galaxies, Centaurus A, ~4.5σ significance

- **promising future:** detector upgrades underway (AugerPrime & TAx4), better composition differentiation, novel machine learning data...

Backup

Best-fit parameters

	Cen A, $m = 0$ (flat)		Cen A, $m = 3.4$ (SFR)		SBG, $m = 3.4$ (SFR)	
	posterior	MLE	posterior	MLE	posterior	MLE
γ	$-0.89^{+0.37}_{-0.33}$	-0.65	$-1.19^{+0.45}_{-0.39}$	-1.41	$-1.02^{+0.43}_{-0.36}$	-1.25
$\log_{10}(R_{\rm cut}/{\rm V})$	$18.20^{+0.04}_{-0.05}$	18.23	$18.21^{+0.04}_{-0.05}$	18.20	$18.24^{+0.04}_{-0.06}$	18.22
f_0	$0.07^{+0.01}_{-0.05}$	0.029	$0.07^{+0.01}_{-0.05}$	0.031	$0.19^{+0.07}_{-0.11}$	0.23
$\delta_0/°$	$30.5^{+2.0}_{-20.2}$	14.4	$27.4^{+4.2}_{-17.0}$	14.3	$18.8^{+5.9}_{-3.6}$	21.9
$I_{\rm H}$	$5.8^{+2.9}_{-2.6} \times 10^{-2}$	4.2×10^{-4}	$1.2^{+0.2}_{-1.2} \times 10^{-2}$	3.0×10^{-4}	$1.2^{+0.1}_{-1.2} \times 10^{-2}$	1.0×10^{-4}
$I_{\rm He}$	$2.7^{+0.4}_{-0.4} \times 10^{-1}$	3.5×10^{-1}	$9.9^{+3.8}_{-2.9} \times 10^{-2}$	1.2×10^{-1}	$1.1^{+0.3}_{-0.4} \times 10^{-1}$	1.4×10^{-1}
$I_{\rm N}$	$5.6^{+0.4}_{-0.4} \times 10^{-1}$	5.0×10^{-1}	$6.7^{+0.7}_{-0.7} \times 10^{-1}$	6.8×10^{-1}	$7.2^{+0.6}_{-0.6} \times 10^{-1}$	7.3×10^{-1}
$I_{\rm Si}$	$9.0^{+3.9}_{-3.4} \times 10^{-2}$	1.4×10^{-1}	$1.5^{+0.5}_{-0.6} \times 10^{-1}$	1.6×10^{-1}	$1.2^{+0.5}_{-0.5} \times 10^{-1}$	9.8×10^{-2}
$I_{\rm Fe}$	$2.3^{+0.9}_{-1.2} \times 10^{-2}$	1.8×10^{-2}	$5.1^{+1.5}_{-1.8} \times 10^{-2}$	4.4×10^{-2}	$4.7^{+1.3}_{-1.7} \times 10^{-2}$	3.8×10^{-2}
ν_E/σ	$-1.24^{+0.68}_{-0.50}$	-1.35	$0.23^{+0.42}_{-0.60}$	0.13	$0.35^{+0.44}_{-0.65}$	0.40
$\nu_{X\,\max}/\sigma$	$-0.94^{+0.29}_{-0.24}$	-0.97	$-1.60^{+0.30}_{-0.25}$	-1.45	$-1.55^{+0.26}_{-0.25}$	-1.33
$\log b$	-254.6 ± 0.1		-264.5 ± 0.2		-258.6 ± 0.2	
$D_{\rm syst}$		2.8		2.1		1.9
D_E ($N_J = 14$)		13.6		21.9		25.3
$D_{X_{\max}}$ ($N_{X_{\max}} = 74$)		107.4		113.6		112.7
D		123.8		137.7		139.9
$\log \mathcal{L}_{\rm ADs}$		9.4		9.5		13.5
$\log \mathcal{L}$		-228.51		-235.3		-232.4

Test statistic

compare likelihood to ref. model (just background sources):

	SBG	**Cen A** *(flat)*	**Cen A** *(SFR)*
$\mathrm{TS}_{\mathrm{tot}}$	25.6	17.3	19.1
TS_E	-4.5	-1.4	-1.1
$\mathrm{TS}_{X_{\mathrm{max}}}$	2.0	0.2	1.0
$\mathrm{TS}_{\mathrm{ADs}}$	27.1	18.7	19.0

SBG model has highest TS = 25.6 ↔ 4.5σ

- including experimental systematic effects
- increase compared to AD-only correlation
- Centaurus region contributes dominant part: **TS~20**
- (E-dependent) arrival directions most important

arrival directions test statistic

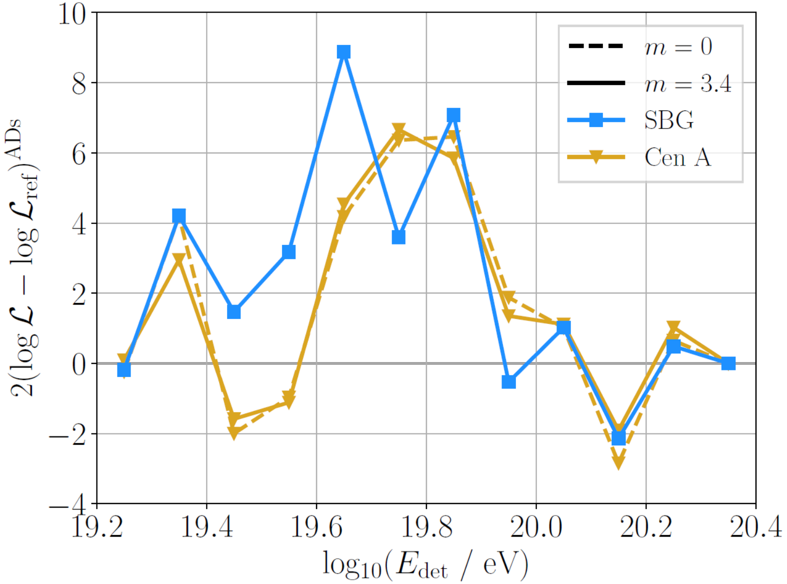

- sum over E bins gives total TS
- peaks could be from He, N, Si
  - but: large uncertainties

Test statistic

	Cen A, $m = 0.0$		Cen A, $m = 3.4$		SBG, $m = 3.4$		γAGN, $m = 5.0$		γAGN+EGMF**, $m = 5.0$	
		+ syst		+ syst		+ syst		+ syst		+ syst
$\mathrm{TS_{tot}}$	22.8	17.3	22.2	19.1	27.6	25.6	23.9*	9.8*	34.3*	33.2*
TS_E	−0.1	−1.4	−0.4	−1.1	−5.2	−4.5	26.8	3.9	18.2	8.4
$\mathrm{TS}_{X_\mathrm{max}}$	1.9	0.2	1.8	1.0	6.2	2.0	−0.8	6.4	4.4	14.7
$\mathrm{TS_{ADs}}$	20.9	18.7	20.8	19.0	26.6	27.1	−2.1	−3.0	11.7	8.6

$$\mathrm{TS_{tot}} = \sum_{\mathrm{obs}=E, X_\mathrm{max}, \mathrm{ADs}} 2(\log \mathcal{L}^{m=x} - \log \mathcal{L}_\mathrm{ref}^{m=x})^\mathrm{obs}$$

$$\mathcal{L}_{X_\mathrm{max}} = \prod_{\tilde{e}} n^{\tilde{e}}! \prod_{x} \frac{(\mu^{\tilde{e},x})^{n^{\tilde{e},x}}}{n^{\tilde{e},x}!}$$

$$\log \mathcal{L}_E = \sum_e \left(n^e \log(\mu^e) - \log(n^e!) - \mu^e\right)$$

$$\mathcal{L}_\mathrm{ADs} = \prod_e \prod_p (\mathrm{pdf}^{e,p})^{n^{e,p}}$$

Bister & Farrar, ApJ 966 71 2024

Dipole direction predictions

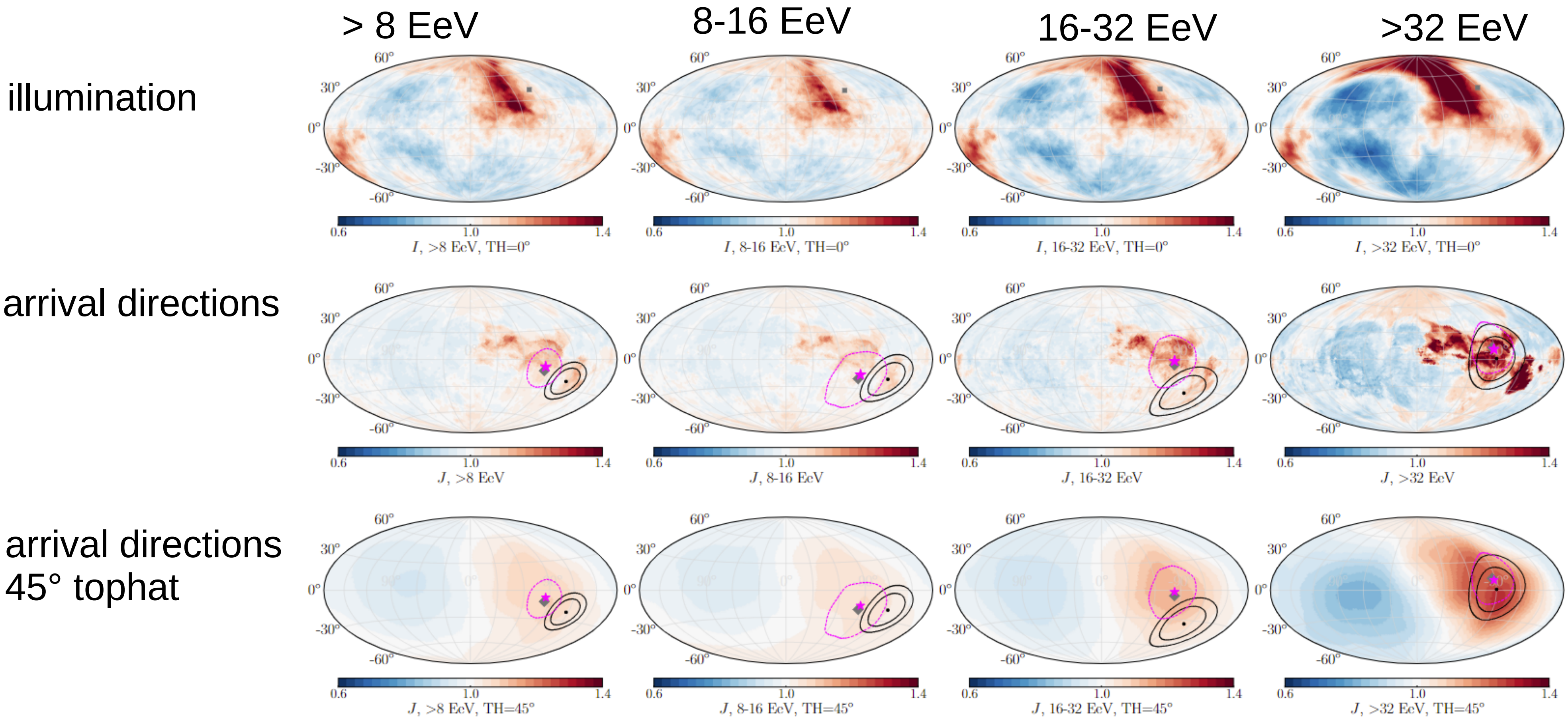

Bister & Farrar, ApJ 966 71 2024

EGMF and transients

$$\delta\theta = 2.9^\circ \frac{B}{\mathrm{nG}} \frac{10\,\mathrm{EV}}{E/Z} \frac{\sqrt{D\,L_c}}{\mathrm{Mpc}} = 2.9^\circ \beta_{\mathrm{EGMF}} \frac{10\,\mathrm{EV}}{E/Z} \sqrt{\frac{\overline{D}}{\mathrm{Mpc}}}$$

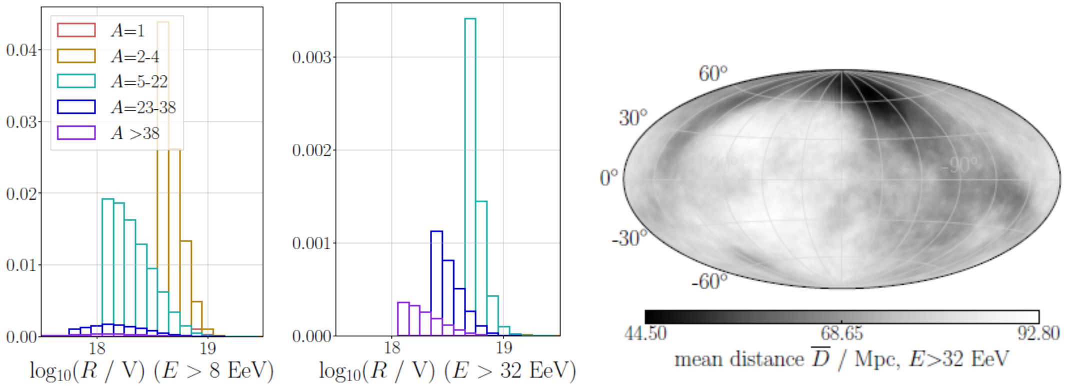

$$n_{\mathrm{eff}} \approx \Gamma\,\tau_{\mathrm{eff}}$$

$$\tau_{\mathrm{eff}} = 0.14 \left(\frac{D}{\mathrm{Mpc}} \frac{\mathrm{EV}}{R} \beta_{\mathrm{EGMF}} \right)^2 \mathrm{Myr} = 34\,\beta_{\mathrm{EGMF}}^2\,\mathrm{Myr}$$

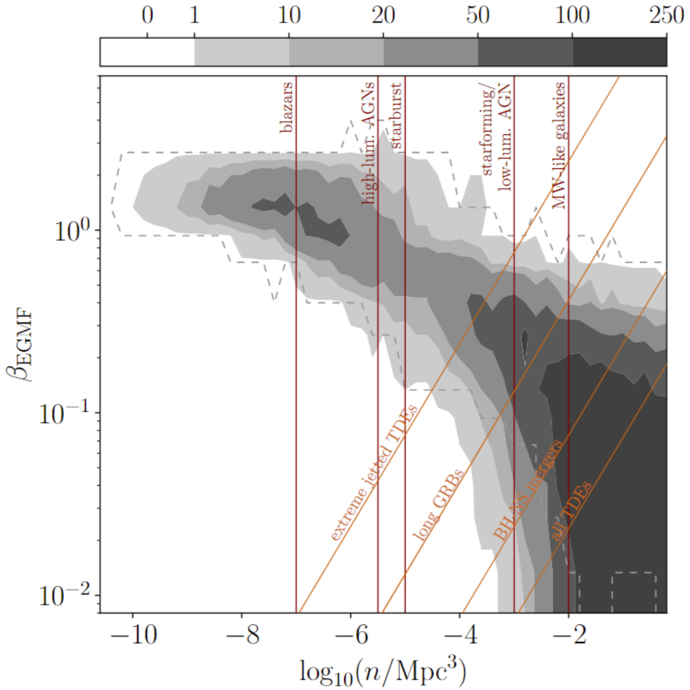

Bister, Farrar, Unger in prep.

UF23 models - which ones are favored?

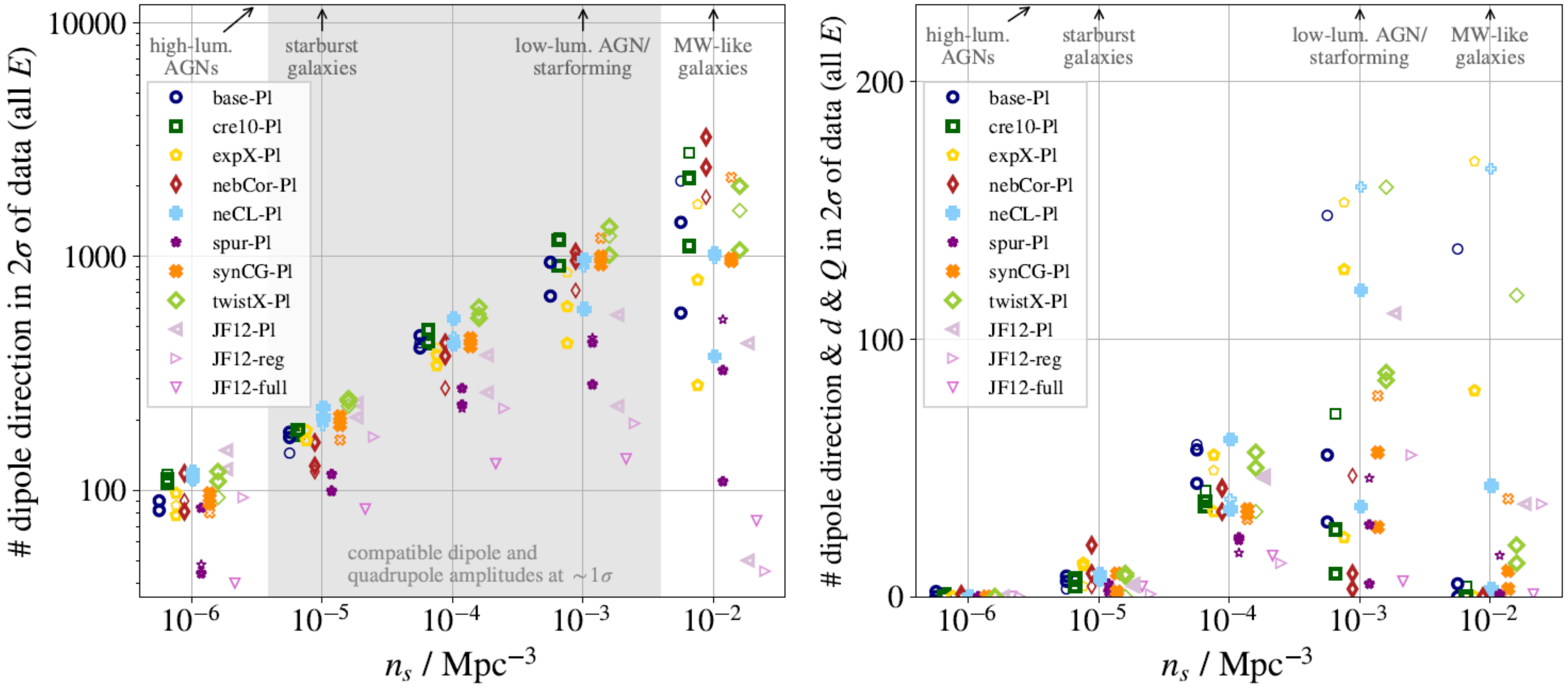

Bister, Farrar, Unger in prep.

UF23 models: EGMF

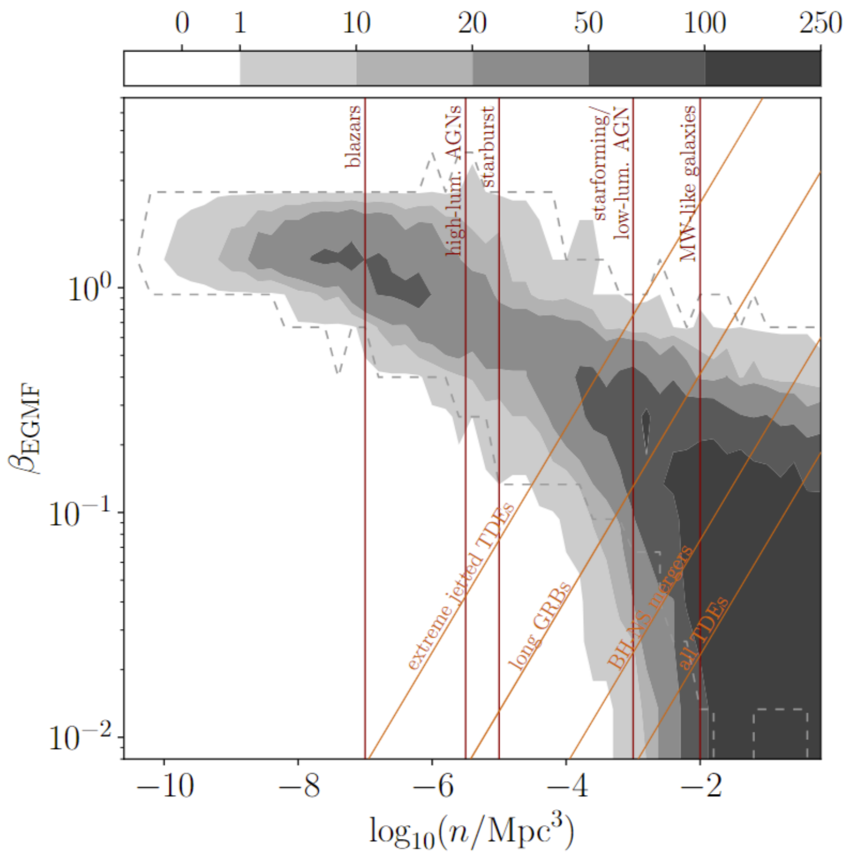

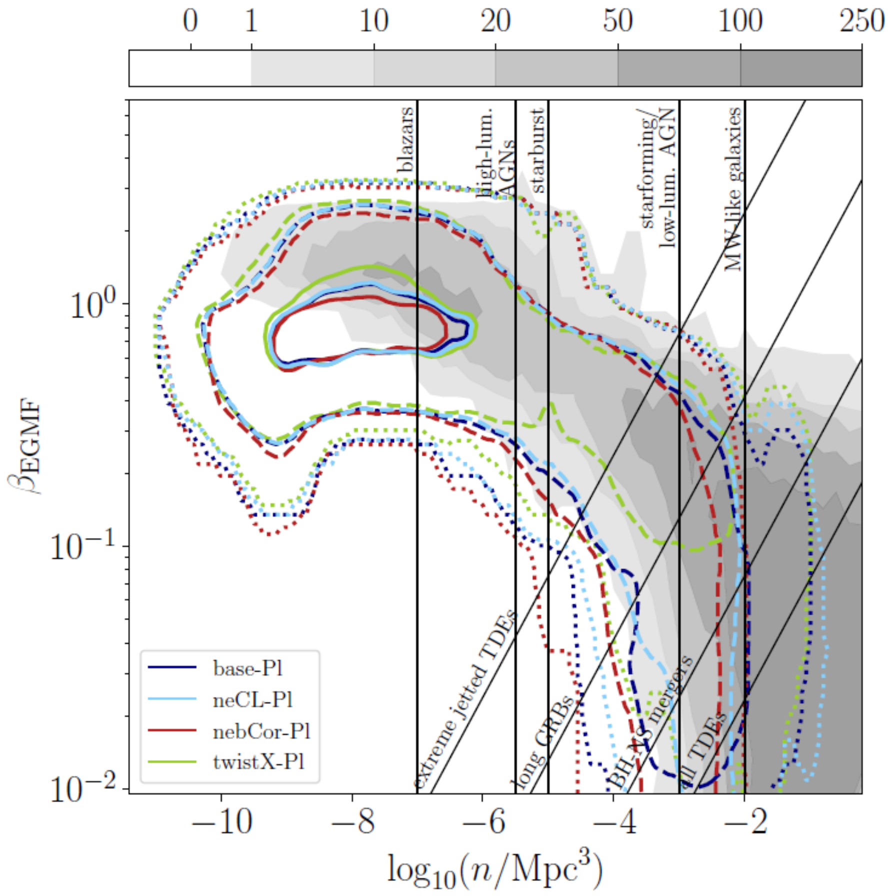

Bister, Farrar, Unger in prep.

UF23 models: dipole & quadrupole

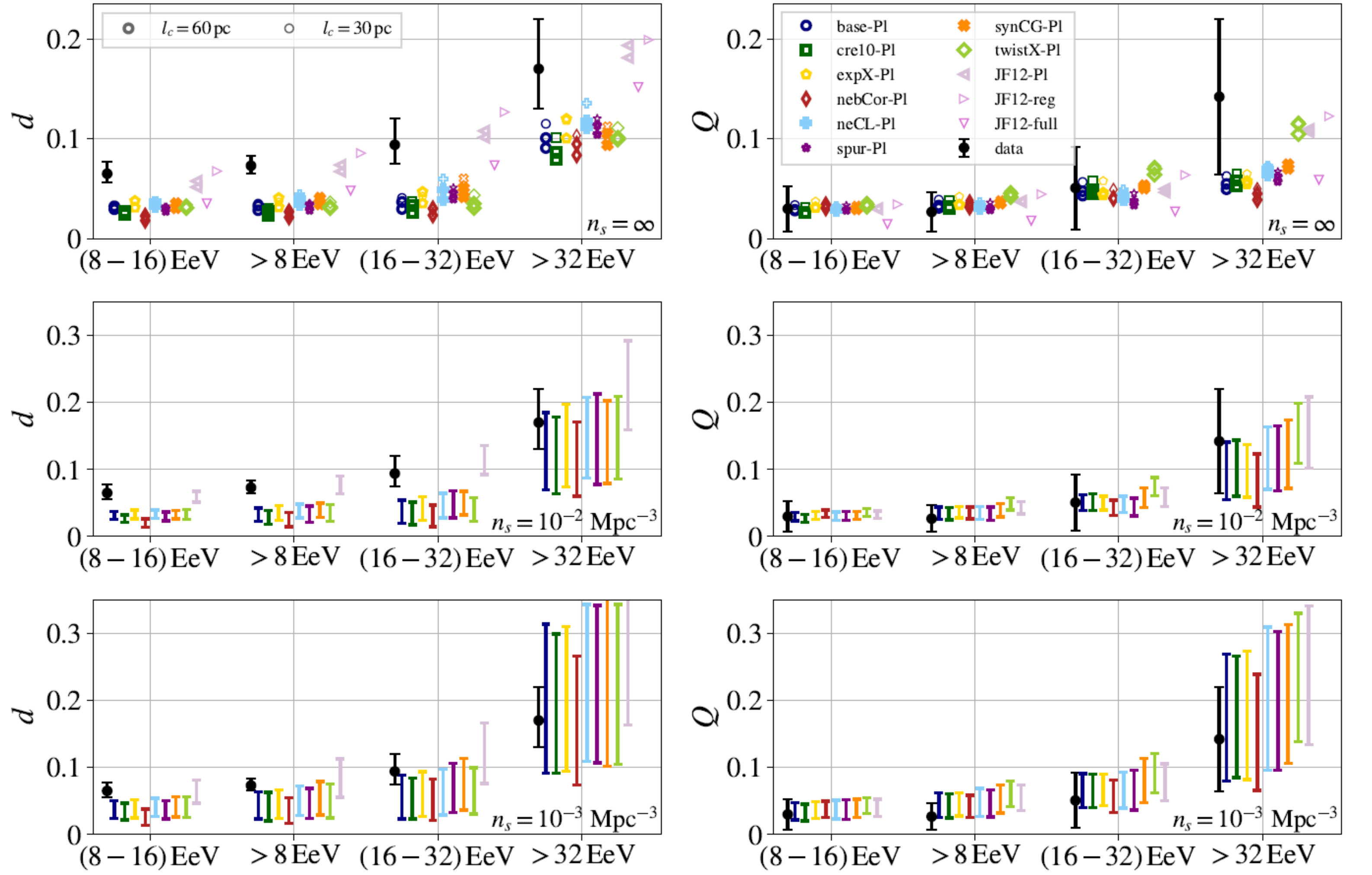

Bister, Farrar, Unger in prep.

UF23 models: dipole & quadrupole

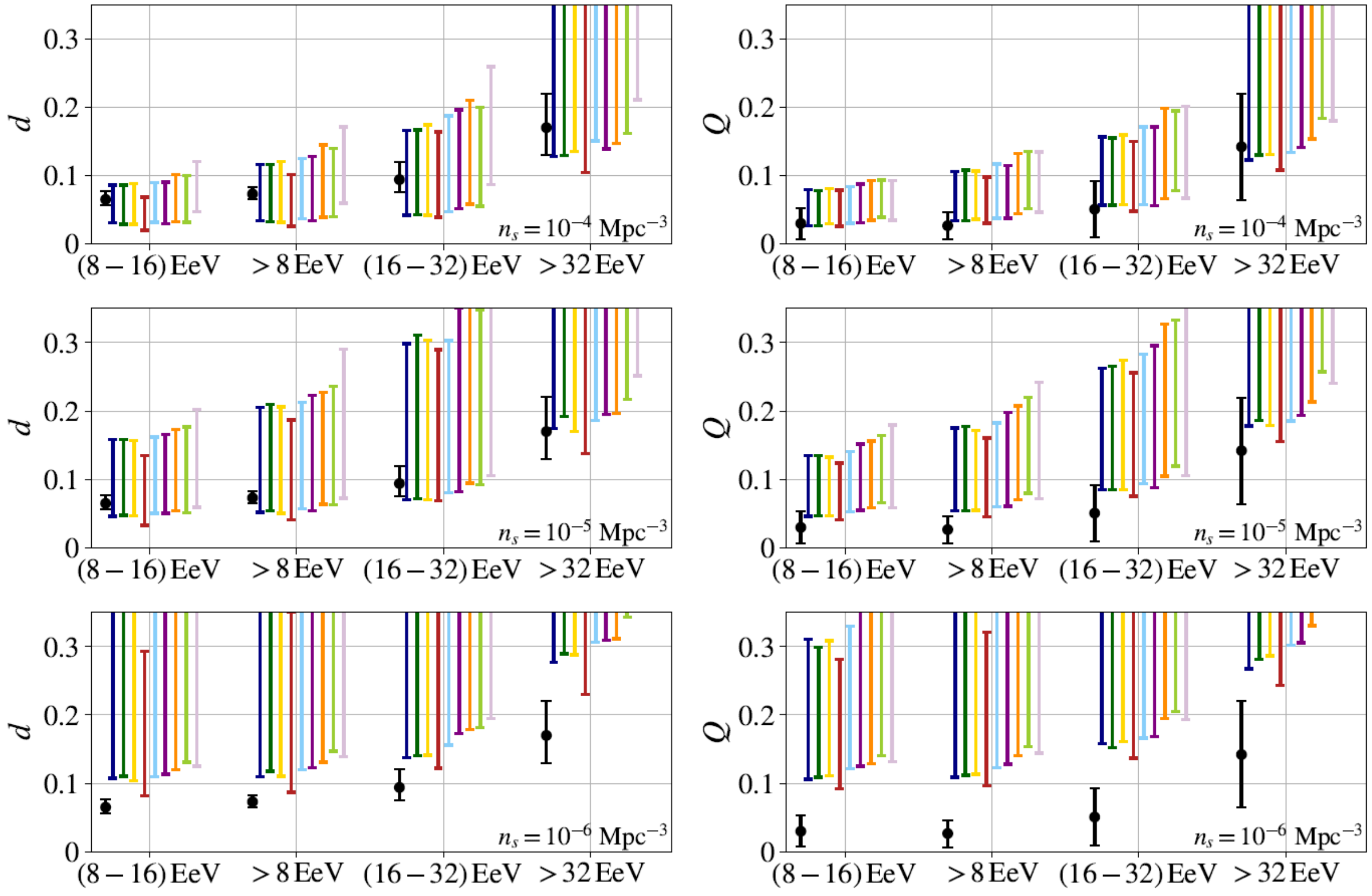

UF23 models: all magnification maps

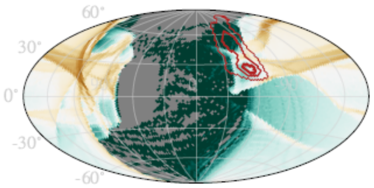

(a) JF12-reg (compare to [30])

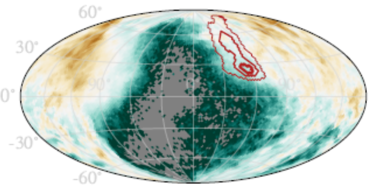

(b) JF12-full $l_c = 30\,\mathrm{pc}$ (compare to [30])

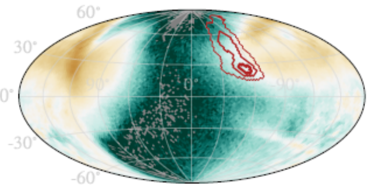

(c) JF12 + Planck $l_c = 60\,\mathrm{pc}$

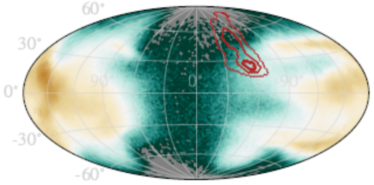

(d) UF23 base + Planck $l_c = 60\,\mathrm{pc}$

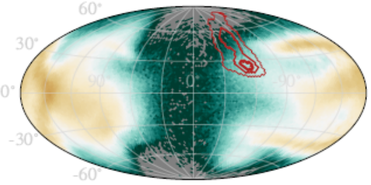

(e) UF23 base + Planck $l_c = 60\,\mathrm{pc}$, 2nd realization

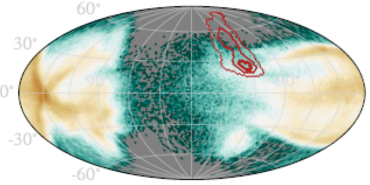

(f) UF23 base + Planck $l_c = 30\,\mathrm{pc}$

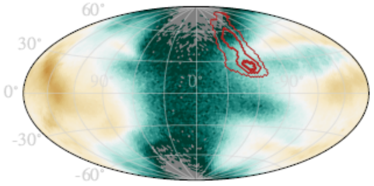

(g) UF23 cre10 + Planck $l_c = 60\,\mathrm{pc}$

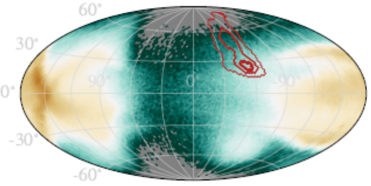

(h) UF23 expX + Planck $l_c = 60\,\mathrm{pc}$

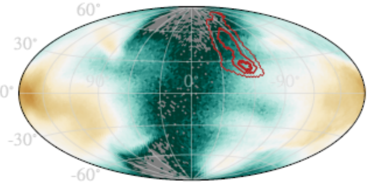

(i) UF23 nebCor + Planck $l_c = 60\,\mathrm{pc}$

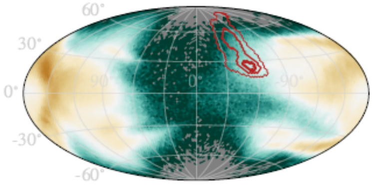

(j) UF23 neCL + Planck $l_c = 60\,\mathrm{pc}$

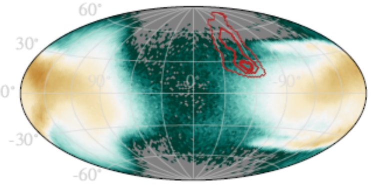

(k) UF23 spur + Planck $l_c = 60\,\mathrm{pc}$

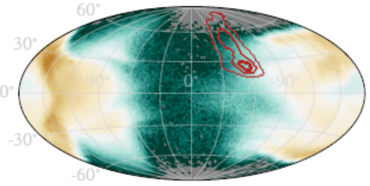

(l) UF23 synCG + Planck $l_c = 60\,\mathrm{pc}$

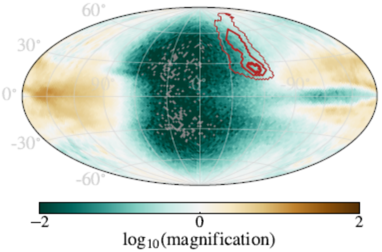

(m) UF23 twistX + Planck $l_c = 60\,\mathrm{pc}$

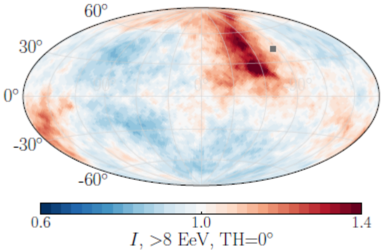

(n) “Illumination” map I from Bister&Farrar (2024)